DOI: 10.1002/ejic.200701047

Colloidal Strategies for Preparing Oxide-Based Hybrid Nanocrystals

Marianna Casavola,[a] Raffaella Buonsanti,[a] Gianvito Caputo,[a] and Pantaleo Davide Cozzoli*[a]

Keywords: Oxides / Nanocrystals / Colloidal synthesis / Surfactants / Topological control / Epitaxial growth / Hybrid nanomaterials

Recent progress of colloidal chemistry in the synthesis of multimaterial nanostructures incorporating transition-metal oxides is reviewed. Attention is focused on the emerging class of hybrid nanocrystals (HNCs), in which domains of different materials are interconnected through inorganic junctions in defined spatial arrangements. The level of expertise so far achieved in the preparation of single-material NCs with finely tuned geometric parameters has been further extended into elegant "seeded growth" approaches for accessing elaborate HNCs by control of interfacial lattice strain and surface energy in liquid media. Various topological configurations are analyzed, including concentric core/shell architectures, hetero-oligomers grouping spherical material domains and more asymmetric hybrid nanostructures based on rod-shaped sections. The chemical-physical properties and technological advantages offered by such multifunctional HNCs are also summarized.

1. Introduction

Colloidal inorganic nanocrystals (NCs) represent one of the most fertile grounds from which the current scientific revolution of nanoscience and nanotechnology is substantially being propelled.[1–5] They are relevant both to the fundamental understanding of the dimensionality-dependent laws of nanosized matter and to the bottom-up development of new functional materials, devices and processes with unprecedented performances. Unlike any other classes of materials, nanoscale transition-metal oxides have increasingly emerged as an exclusive platform where diverse optoelectronic, magnetic, thermal, mechanical, electrochemical and catalytic properties can coexist with the potential for low-cost and environmentally safe technologies.[6,7] At the nanoscale, unique effects such as surface- and strain-driven lattice distortion, variation in electronic state density and oxidation-induced charge redistribution systematically evolve with size and jointly impact on the structural-mechanical stability, the magneto-optoelectronic response and the chemical reactivity of nanostructured oxides.[6,8–11] These contributions attribute an exceptionally wide range of properties, which cover almost all aspects of materials science and solid-state physics, to oxide NCs. For these reasons, these compounds have found numerous applications, for example as adsorbents for air/water purification and fuel treatments, in photovoltaic and photoelectrochemical devices, in gas sensing, in photocatalytic removal of pollutants, in fuel cells, in the realization of advanced ceramics, in self-cleaning, antifogging and antibacterial functional coatings, and in biomedicine.[6,7,12–17]

Among the various wet-chemistry approaches to nanostructures, surfactant-assisted chemical approaches have been especially distinguished for their capability to provide finely size- and shape-tailored NCs of semiconductor, oxide and metal materials by careful regulation of thermodynamically and kinetically driven growth processes in liquid media.[2,3] While refinement of this synthetic expertise is far from being exhausted, further efforts are currently pursued to fabricate novel NCs with a higher level of structural and compositional complexity and, consequently, of functionality. In recent years, nanochemistry research has seen tremendous advances with the solution-phase synthesis of first generations of so-called hybrid nanocrystals (HNCs) with a topologically controlled distribution of their composition.[4,18] These are structurally elaborated multimaterial NCs, consisting of two or more chemically different material sections interconnected through permanent inorganic interfaces. The technological horizons that these HNCs can potentially span are incredibly extensive. First, the fusion of luminescent, magnetic and catalytic sections without bridging molecules or embedding matrices yields individually processable particles in which different properties are simultaneously available. This allows many fields of application (e.g., biomedicine, environmental clean-up, catalysis, sensing, composite material fabrication), which demand for "smart" platforms able to accomplish multiple tasks (e.g.,

[a] National Nanotechnology Laboratory of CNR-INFM, Unità di Ricerca IIT, Distretto Tecnologico ISUFI,
Via per Arnesano Km 5, 73100 Lecce, Italy
Fax: +39-0832-298238
E-mail: davide.cozzoli@unile.it

possibility of parallel targeting, detection and therapy action in living systems), to benefit from multifunctionality in a straightforward way. Second, as a result of the electronic contact that is established across adjacent material domains, HNCs can display strongly modified or even unexpected physical-chemical responses, compared to those normally exhibited by the individual components. This suggests that forming an intimate junction among different size- and shape-controlled NC portions can be exploited as an additional tool to engineer their performances. Third, in HNCs, exchange coupling mechanisms among magnetic, optical and electrical properties can be operative, allowing for the investigation of novel spintronic phenomena stemming from coupled effects in individual nanoheterostructures.

In this review, we will illustrate surfactant-assisted strategies that have been recently devised to synthesize topologically controlled HNCs, keeping a focus on those which incorporate oxide materials. We will show how the ability to prepare monomaterial NCs with finely tuned geometric parameters has been further extended into elegant "seeded growth" approaches for accessing multimaterial HNCs by controlling interfacial lattice strain and surface energy in liquid media. Various topological configurations will be analyzed, including centrosymmetric core/shell architectures, hetero-oligomers grouping spherical material domains and nonconcentric nanoheterostructures with high spatial asymmetry based on anisotropically shaped material sections. The properties and technological advantages offered by such newly conceived generations of complex nanocrystals will also be summarized.

2. General Concepts in Surfactant-Assisted Synthesis

2.1 Single-Material Nanocrystals

Colloidal NCs are synthesized in solution in the presence of some stabilizing organic agents, broadly termed as surfactants. As extracted from their growing medium, NCs typically comprise a crystalline core with the desired chemical composition, which is responsible for their inherent chemical-physical properties, and a monolayer of tightly bound capping molecules, which impart solubility and colloidal stability to the particles. The technological convenience of colloidal NCs over traditional types of nanostructures resides in two aspects. First, their production can be cheaply scaled up to milligram-to-gram quantities for many

Marianna Casavola was born in Bari, Italy, in 1978. She received her MSc degree in Chemistry from the University of Bari, Italy, in 2005. During her graduate research, she worked on the plasma-assisted deposition of Ag/PEO-like nanocomposites as antibacterial coatings. Since 2006, she has been working as a PhD student at the National Nanotechnology Laboratory of CNR-INFM, Lecce, Italy. Her research project involves the development of metal-oxide-based hybrid nanocrystals for photocatalytic and magnetic applications.

Raffaella Buonsanti was born in Matera, Italy, in 1981. She received her MSc degree in Chemistry from the University of Bari, Italy, in 2006. Her graduate research was focused on the colloidal synthesis and characterization of nanocrystal heterostructures based on magnetic and photocatalytically active oxides. Since 2007, she has been working as a PhD student at the National Nanotechnology Laboratory of CNR-INFM, Lecce, Italy. Her research activities include the preparation, characterization and biological applications of complex semiconductor–magnetic hybrid nanocrystals.

Gianvito Caputo was born in Mola di Bari, Italy, in 1977. In 2005 he received his MSc degree in Chemistry from the University of Bari, Italy. During his graduate thesis work, he studied the mechanical properties of oxide and nitride thin films deposited by plasma-assisted techniques. Since 2006, he has been carrying research activities as a PhD student at the National Nanotechnology Laboratory of CNR-INFM, Lecce. He is involved in the synthesis of oxide nanocrystals and their use in the fabrication of organic–inorganic nanocomposite systems with tailored optical, mechanical and wettability properties.

Pantaleo Davide Cozzoli was born in Brindisi, Italy, in 1975. He received his MSc degree in Chemistry in 1999 from the University of Bari, Italy, and his PhD in Chemical Sciences from the same institution in 2004, defending a dissertation on the synthesis and photocatalytic applications of shape-controlled oxide nanocrystals. He spent part of his PhD at the University of Hamburg (Germany). From 2005 to 2007 he has worked as a postdoctoral fellow at the National Nanotechnology Laboratory (NNL) of CNR-INFM, Lecce, Italy. Presently, he holds a permanent position as staff research scientist at the Scuola Superiore ISUFI of the University of Lecce, in association with NNL. His research interests focus on the chemical engineering, characterization and multipurpose applications of elaborate semiconductor, metal and magnetic colloidal nanocrystal heterostructures.

materials by using a relatively inexpensive equipment. Second, they are surface accessible, which allows them to be processed and implemented into disparate technologies.

Surfactant-assisted syntheses have largely proven to be the most powerful wet-chemistry tools to tailor the size, shape and composition of inorganic NCs.[2,3,5] Indeed, judicious adjustment of a few experimental parameters, such as the type and the relative concentration of molecular precursors and organic stabilizers, in combination with temperature, transcribes into a control over a number of complex phenomena occurring during crystal formation in liquid media, including solution supersaturation, reactant diffusion, relative stability of crystal polymorphs and crystallographic-direction-dependent growth rates.[2,3,5] The general scheme of a colloidal synthesis involves reactions of organometallic precursors (that carry the atomic species necessary to build the desired material) in the presence of specific surfactant molecules (e.g., alkylamines, thiols, carboxylic and phosphonic acids, phosphanes, phosphane oxides, etc). Once the synthesis is activated, highly reactive species are generated, commonly referred to as the "monomers", which induce the nucleation of NCs and sustain their subsequent enlargement. The surfactants play several key roles during the synthesis. Indeed, they form complexes with the monomers, thereby tuning their reactivity, while they simultaneously participate in an adsorption/desorption dynamics at the surface of the growing clusters, which prevents them from aggregation and uncontrolled growth. Mechanistic studies have shown that monodisperse NCs are produced when a short burst of nucleation, that enables temporal separation of the nucleation and growth processes, is combined with a diffusion-controlled growth process. Satisfactory tailoring of the NC size and size-distribution can be achieved by balancing the relative depletion of monomers between the nucleation and growth stages with the aid of suitable techniques (e.g., the "hot injection"), by profiting from the particular reactivity of the system (e.g.; "delayed nucleation") or by exploiting digestive ripening.[2,3,5] It is also worth mentioning that surfactants can affect the specific surface energy of the growing NCs, which has important implications in the tuning of their shape.[2–4] Indeed, facet-preferential ligand adhesion can modify the relative growth rates along the various crystallographic directions and/or can favour the selective elimination of unstable surfaces by triggering oriented attachment of particles. In the absence of additional circumstances that can interrupt growth symmetry (e.g., formation of nonspherical soft micelle templates, the presence of foreign particle catalysts or the application of external electric or magnetic fields), surfactants remain mostly responsible for the formation of NCs in a variety of anisotropic shapes, such as cubes, polyhedrons, rods, wires, polypods and rings.[4]

2.2 Multimaterial Hybrid Nanocrystals

The most recent developments of colloidal techniques involve elegant extensions of the above-mentioned surfactant-assisted strategies to the fabrication of more elaborate hybrid nanocrystals (HNCs). The most widely exploited solution-based techniques for the synthesis of HNCs rely on a simple principle of the Classical Nucleation Theory (CNT), according to which the activation energy for the enlargement of pre-existing particles in a solution (i.e., heterogeneous nucleation/growth) is considerably lower than the barrier for the generation of novel nuclei (i.e., homogeneous nucleation).[19–21] This concept has been exploited in a simple and general reaction scheme, which is referred to as "seeded growth". In this scheme, preformed NCs of one material (i.e., the "seeds") are already present or are introduced into a solution environment containing the molecular precursors that are necessary to build a second different material. Under suitable reaction conditions, the latter can preferentially deposit and grow onto the seeds, rather than nucleating homogenously. Despite the apparent simplicity of this strategy, the preparation of HNCs in liquid media requires an exceptionally higher degree of synthetic expertise. In fact, the CNT takes into account neither growth con-

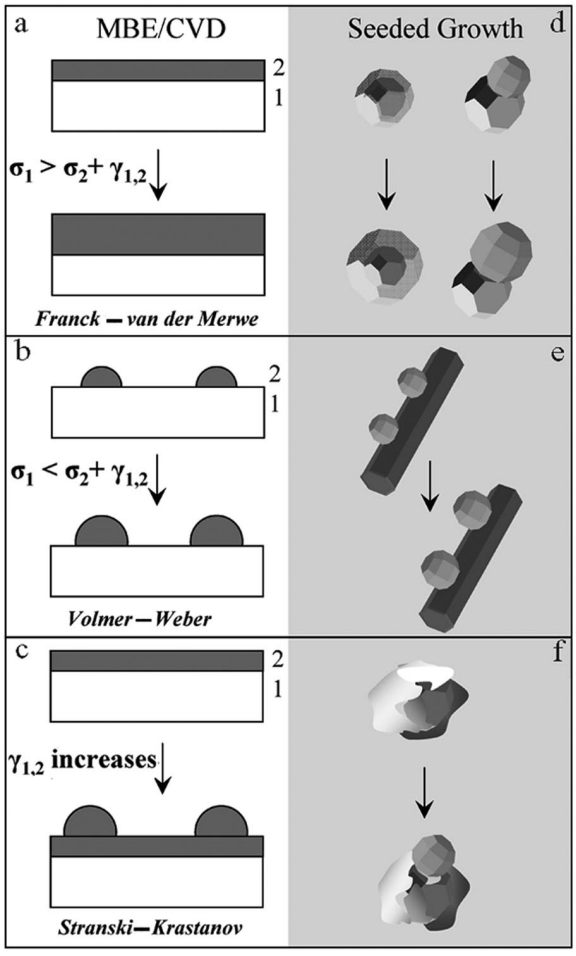

Scheme 1. Comparative sketches illustrating heterogeneous growth modes accomplished by: MBE/CVD techniques (a–c); "seeded growth" approaches in the solution phase (d–f).

straints related to lattice incompatibility nor changes in the liquid/solid interface tension induced by adhesion of surfactants to the growing clusters. Therefore, in the preparation of nanoheterostructures comprising structurally dissimilar materials, the thermodynamic and kinetic processes, which influence the size and shape of the individual domains, are further complicated by material miscibility, interfacial strain and facet-dependent chemical reactivity. In order to understand such a complex growth dynamics, it is helpful to consider that the creation of hybrid NC-based architectures by seeded growth in the solution phase is closely analogous to the more traditional heteroepitaxial deposition processes accomplished by the Molecular Beam Epitaxy (MBE) and Chemical Vapour Deposition (CVD) techniques, which have been widely exploited for the fabrication of semiconductor and magnetic heterostructured systems (e.g., sandwiched multilayer structures, quantum dots or quantum wells) starting from gaseous precursors.[21–23] Indeed, the way in which two materials attain an inorganic heterointerface is ultimately related to the fulfilment of the same fundamental energy requirements. This parallelism is illustrated in Scheme 1. Consider a material substrate with a well-defined crystallographic orientation (referred to as "1" in the scheme), onto which a second material (labelled as "2") is allowed to grow. The change in the total surface energy, $\Delta\gamma$, that accompanies the overall deposition process is given by Equation (1):

$$\Delta\gamma = \sigma_1 - (\sigma_2 + \gamma_{1,2}) \quad (1)$$

where σ_1 and σ_2 are the surface energies of the respective materials, and $\gamma_{1,2}$ is the solid–solid interfacial energy, which is mostly related to the mismatch-induced strain between the two lattices. The growth mode that will be adopted in a given system will depend on the balance between these terms. When the material to be added is characterized by a lower surface energy ($\sigma_2 < \sigma_1$) and good lattice fit (i.e., $\gamma_{1,2}$ is low) with respect to the substrate, such that $\Delta\gamma > 0$, then the deposition can proceed layer-by-layer toward a uniform coverage (Scheme 1a: *Frank–van der Merwe* mode). When the foreign material possesses a high surface energy ($\sigma_1 < \sigma_2$) and/or it is significantly lattice-mismatched (i.e., $\gamma_{1,2}$ is high), such that $\Delta\gamma < 0$, then its deposition can take place only by the formation of island-like features (Scheme 1b: *Volmer–Weber* mode). An additional possibility includes a mixed deposition regime, in which growth initially occurs layer-by-layer and then continues by producing islands in response to a sudden increase in interfacial strain along the course of the deposition (Scheme 1c: *Stranski–Krastanov* mode). All of these growth regimes can be equally transcribed to the context of a seeded growth of HNCs, whereby the initial nanocrystal seeds act as the substrate for deposition of a foreign material in the solution phase. For instance, if the conditions for complete wetting were satisfied either for any one of the facets exposed by a starting seed or selectively for only one or a few of them, the resulting HNCs could assume an onion-like or a dimer-/oligomer-like configuration, respectively (Scheme 1d). On the other hand, under an incomplete wetting regime, HNCs for which one or more sufficiently extended facets of the original seeds are decorated with multiple domains of the new material (Scheme 1e) could originate. As an intermediate case, transitions from metastable onion-like type architectures to phase-segregated nonconcentric heterostructures could be expected as a convenient means of lowering the interfacial strain (Scheme 1f).

It deserves emphasis that the creation of nanoscale heterointerfaces in colloidal solutions can benefit from the possibility of modulating the solution/solid interfacial tension (i.e., σ_1 and σ_2) by means of organic surfactants, an opportunity that is prohibited to MBE/CVD techniques. Indeed, the outstanding results that have been so far reported have highlighted that HNCs made of a given combination of structurally dissimilar materials can be accessed in more than one topological arrangement, whereby the interface energy term is properly balanced by the surface energy contributions. Moreover, in the liquid-phase synthesis, the growth of HNCs can be accompanied by unexpected or unusual mechanisms (not fully understood yet) through which misfit-induced interfacial strain can be accommodated (e.g., by local curving of near-interface junction planes) or compensated for (e.g., by a decrease in the total surface energy due to solvent or surfactant binding, or by elimination of unstable facets due to interface formation). This may lead to heteroepitaxial interfaces with low defect density, which is of paramount importance when aiming at reproducible properties and enhanced exchange coupling effects.[24]

3. Heterostructures in Centrosymmetric Core-Shell Configuration

The most common topology in which oxide-based HNCs have been reported is the so-called core@shell geometry, in which a NC is uniformly enveloped by a layer of another material, which usually reproduces the symmetry of the inner core. As a general advantage, associations of various semiconductors, metals and oxides in onion-like configurations often exhibit distinct behaviour as compared to that inherent to the individual components, such as tunable optical and magnetic properties or enhanced catalytic activity, depending on the specific combination.

Core@shell HNCs with epitaxially fused core and shell sections can form when the materials involved have similar crystal structure and lattice parameters (with differences of the order of 1–3%), so that the overall structure experiences negligible strain as long as the coating thickness is small enough. Nevertheless, when the synthesis conditions allow the interfacial energy to be somewhat counterbalanced by a proportional decrease in surface energy [see Equation (1)], then the requirements of lattice compatibility can be fairly less restrictive.

Colloidal strategies for accessing core@shell HNCs have proliferated in the last decade. They can be classified into three main typologies, all of which can be regarded as variants of the general seeded growth scheme: (a) direct hetero-

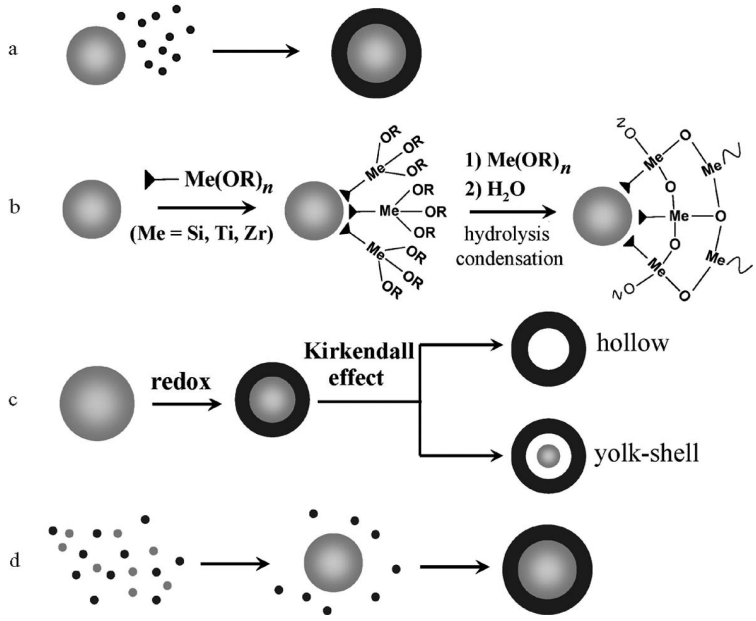

Scheme 2. Sketch of mechanisms leading to the formation of core@shell HNCs: (a) direct heterogeneous nucleation and growth of the shell material onto preformed nanocrystal cores; (b) shell growth after chemical activation of the core surface; (c) sacrificial redox replacement of the core surface followed by vacancy coalescence; and (d) self-controlled nucleation growth.

geneous nucleation and growth of the shell material onto preformed nanocrystal cores; (b) shell growth after chemical activation of the core surface; (c) sacrificial redox replacement of the core surface; and (d) one-pot approaches by self-controlled nucleation growth. These mechanisms are sketched in Scheme 2a–d.

3.1 Direct Heterogeneous Nucleation and Growth of the Shell

Disparate classes of core@shell structures have been obtained by selective heterogeneous nucleation and growth of a layer of a second material on preformed nanocrystal seeds (Scheme 2, path a). Strategies for achieving this goal aim at circumventing parasitic homogeneous nucleation of the shell material by performing a slow addition of the relevant molecular precursors to the cores under mild temperatures and/or by delicately controlling the reactivity of the system by ligands. A representative transmission electron microscopy (TEM) image gallery of core@shell HNCs obtained by this mechanism is reported in Figure 1.

Metal@oxide HNCs, where the core is made of either Au or Ag and the shell is composed of TiO_2, ZrO_2 or SnO_2, have been grown in mixed organic/aqueous media by combining a metal salt reduction with sol–gel reactions for oxide network formation. The general two-step procedure involves accomplishing hydrolysis-condensation of transition-metal-alkoxide precursors in the presence of surfactant-capped metal NCs, provided by an independent synthesis. In this way, shells with either a smooth[25] or a flower-like morphology[26,27] are obtained (see, for example, Figure 1a–b). Except for the case in which a harsh hydrothermal treatment is applied during oxide formation, all the aforementioned routes typically yield amorphous coatings, which often exhibit discontinuities, nanoporosity and/or even inner cavities. Profiting from the chemical accessibility of their inner cores, these metal@oxide HNCs have been exploited as catalytically active nanoreactors,[29] as efficient electronic capacitors,[28] as well as sacrificial templates for the creation of hollow oxide capsules upon selective metal oxidation.[29,30] In addition, these systems reveal shell-tuneable surface plasmon absorption and interesting nonlinear optical properties with a high laser damage threshold.[25,28]

Another class of core@shell structures that have been obtained by this scheme is represented by oxide@metal HNCs, which normally combine ZnO or TiO_2 with Au, Ag, Pt or Cu. Typical preparations start from an alcohol suspension of weakly organic-passivated oxide NCs on which either chemical[31–34] or oxide-photocatalyzed reduction[35–36] of the desired metal precursors is accomplished. Depending on the specific experimental conditions used, the deposition process can achieve various degrees of surface coverage, leading to oxide NCs decorated with small island-like metal patches or entirely coated by a shell of irregular thickness. The pronounced light sensitivity of such noble metal nanostructures has been verified in laser irradiation experiments, during which initially well-separated oxide@metal HNCs undergo photoinduced fusion into larger composite structures, each comprising multiple oxide domains embedded in a metal matrix.[33] Although detailed information on the shell structure has not been provided for such nanostructures, the attainment of a semiconductor/metal nanojunction has been proven to have a remarkable impact on the applications of these HNCs in solar energy harvesting. Indeed, under bandgap photoexcitation of the semiconductor section, the metal component

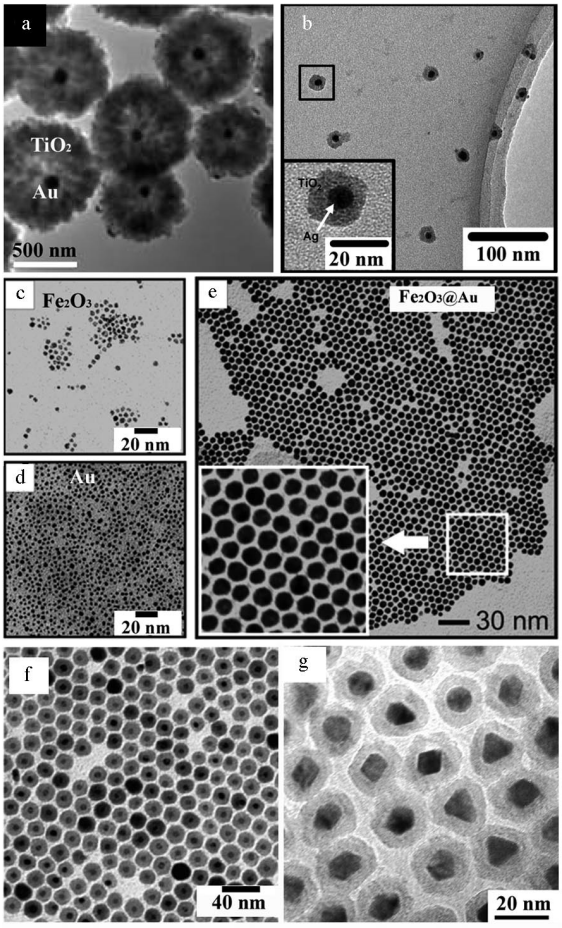

Figure 1. Examples of core@shell HNCs synthesized by direct heterogeneous nucleation and growth of the shell material onto preformed nanocrystal cores. Low-magnification transmission electron microscopy (TEM) images of: (a) Au@TiO_2 nanoreactors with inner vacant space (reproduced in part from ref.[27] with permission, copyright Wiley-VCH Verlag GmbH & Co. KGaA); (b) Ag@TiO_2 HNCs (reproduced in part from ref.[25] with permission, copyright 2006 American Chemical Society); (c–e) Fe-oxide@Au HNCs (e) obtained by thermally induced coalescence of Au NCs (d) onto Fe-oxide seeds (c) (reproduced in part from ref.[40] with permission, copyright 2007 American Chemical Society); (f) Au@Fe_3O_4 HNCs (reproduced in part from ref.[43] with permission, copyright 2006 American Chemical Society); (g) Pt@Fe_3O_4 HNCs (reproduced in part from ref.[45] with permission, copyright IOP Publishing).

acts as a sink for the photogenerated electrons, thereby circumventing their recombination with holes. The altered carrier separation dynamics in such HNCs can be advantageously manipulated in order to benefit from either higher photocatalytic reaction yields or enhanced charge storage capability under equilibration of the Fermi levels of two materials, as well as modulate the metal surface plasmon absorption.[31–36]

A few attempts to form core@shell associations of two semiconductors have been also reported. They involve the coupling of ZnO with CdSe or CdS.[37,38] These HNCs are appealing candidates for photovoltaic and photocatalytic applications, since relative band edge staggering of the component materials is such that the cadmium chalcogenide works as a sensitizer for the oxide in the visible range. One example is represented by ZnO nanorods decorated with irregularly shaped crystalline CdS domains that have been grown by ultrasonication of aqueous suspensions containing oxide seeds, $CdCl_2$ and thiourea.[37] This method enables only a rather limited control over the heterostructure topology, as CdS nucleation is not site-specific. Although neither mechanistic aspects nor the involved epitaxial relationships have been clarified, the superior transport and gas-sensing properties of these ZnO@CdS HNCs relative those of ZnO alone suggest that good electronic connection should exist between the two materials. These findings are likely to encourage the design and fabrication of high-performance optoelectronic devices based on colloidal semiconductor oxide nanoheterostructures.[37]

A reversed configuration has been claimed with the synthesis of CdSe@ZnO HNCs through an approach that somewhat resembles a phase-transfer procedure.[38] Highly hydrophobic, surfactant-capped CdSe seed NCs (which are soluble in nonpolar media) are mixed with an alcohol solution of zinc acetate under ultrasonication, which favours detachment of the native ligands and subsequent adsorption of the zinc monomer species. This surface-activating process of the CdSe seeds is found to be critical to guarantee the growth of a ZnO layer upon hydrolysis of the precursor. Since acetate moieties now protrude out of the ZnO shell into the solution, the ZnO-coated CdSe cores are ultimately rendered dispersible in the polar alcohol medium.[38] As an indirect proof for the formation of a core@shell structure, an increase in the photoluminescence quantum yield of CdSe has been reported; however, no further structural confirmations have been supplemented.

Another interesting category of bifunctional HNCs is represented by core@shell nanostructures in which a layer of a noble metal, such as Au or Ag, surrounds a magnetic interior made of iron or iron oxide.[39–42] A key advantage of these Fe/Fe-oxide@metal HNCs resides in the association of a biocompatible core, which is potentially useful as an MRI (magnetic resonance imaging) contrast agent or is exploitable in magnetically driven separations, with an optically active surface that is easy to functionalize. Several routes to Fe-oxide@metal HNCs have been devised, as summarized in the following discussion.

In one approach, organic-capped Fe_3O_4 NCs, prepared nonhydrolytically, act as substrates for the alkyldiol reduction of gold acetate in the presence of oleic acid (OLAC) and oleylamine (OLAM) at ca. 180 °C.[39] A high temperature is needed to regulate the adsorption/desorption dynamics of the surfactant on the Fe_3O_4 surface of the seeds, so as to render them accessible to the reactive gold species. An appealing variant of this procedure relies on the thermally induced fusion of presynthesized OLAC/OLAM-capped Fe_3O_4 and thiol-capped tiny Au NCs codissolved in toluene in the presence of an ammonium bromide salt.[40] During the heating of this mixture at 150 °C in a closed vessel, the less stable Au NCs selectively attach to the Fe_3O_4 NCs and coalesce, forming a uniform metal coverage on such seeds (Figure 1c–e). This evolution can be rationalized by con-

sidering that the fusion of such tiny Au clusters can reduce the overall surface energy of the heteroparticle system. Both of the aforementioned routes have been demonstrated to lead to rather monodisperse Fe_3O_4@Au HNCs, which, however have been characterized mainly in-ensemble rather than individually. The attained core@shell configuration has been indirectly assessed by comparing elemental analysis data for as-prepared HNCs and for HNC thin films deposited on glass substrates by gold-selective dithiol-mediated assembly.[39,40]

Room-temperature aqueous syntheses have been also reported, although the quality of the resulting nanostructures in terms of size distribution and control over the degree of aggregation is inferior. Water-soluble γ-Fe_2O_3@Au HNCs have been obtained by hydroxylamine reduction of a gold salt in aqueous tetrabutylammonium-stabilized suspensions of oxide NCs.[41] In another approach to Fe_3O_4@Ag HNCs, water-in-oil microemulsion droplets have been used to confine the reaction of silver nitrate with borohydride in the presence of suspended Fe_3O_4 NCs.[42] In both cases, the seeds are only weakly surface-passivated, so that the deposition of a rather thick shell can occur under mild conditions. Occasionally, structures made of multiple cores embedded within a single shell matrix have been detected.[40,41]

Fe-oxide@metal HNCs exhibit the characteristic surface plasmon absorption of nanosized Au/Ag that correlates with the shell thickness.[39–41] As for their magnetic properties, lower blocking temperatures and higher coercive fields have been measured relative to those found for the corresponding Fe_3O_4 cores, which has been explained by a decreased coupling of the particle magnetic moments due to the screening effect of the metal shell. Notably, the versatile surface chemistry of gold and the magnetism of iron oxide have paved the way to prototypical biological applications of these hybrid nanostructures after water transfer and shell functionalization with proteins, such as in bioassays and magnetic-field-assisted separation.[40] The potential of Fe_3O_4@Ag HNCs as recyclable antibacterial agents has also been proven.[42]

A set of inverted metal@Fe-oxide HNCs has also been devised by heterogeneous nucleation/growth seeded approaches.[43–45] Monodisperse Au@Fe_3O_4 HNCs with either spherical or cube-like shells and good epitaxial connection between the two materials (see, for example, Figure 1f) have been synthesized by a two-stage strategy relying on the thermal decomposition of $Fe(CO)_5$ at 200–300 °C in alkyl ether solvents in the presence of small Au seeds and OLAC/OLAM surfactants.[43] These heterostructures are characterized by a pronounced red-shift of the Au plasmon resonance due to dielectric coating effects and by an increased magnetic coercitivity due to extra surface anisotropy, both of which clearly manifest interactions between the two materials. By using a growing environment analogous to that described above, highly regular Pt@γ-Fe_2O_3 HNCs have been obtained by one-pot sequential synthesis in an OLAC/OLAM/octyl ether mixture at 290 °C, in which Pt NCs are first nucleated in-situ upon alkyldiol reduction of platinum acetylacetonate and subsequently combined with the iron precursor for shell growth.[44] The relative geometric parameters of the HNCs are easily engineered by adjusting the relative reactant concentration ratio (Figure 1f). The Pt@γ-Fe_2O_3 HNCs have been converted by a high-temperature solid-state reaction under a H_2/Ar atmosphere into bimagnetic Fe_xPt_{1-x}@Fe heterostructures possessing exchange-coupled soft and hard phases as well as high coercitivity, which are appealing features from the perspective of building permanent hard magnets and data storage media.[45]

Bimagnetic FePt@MFe_2O_4 HNCs (where M = Fe, Co) with a coherent core/shell interface have also been accessed directly by a two-step, surfactant-assisted solution synthesis.[46,47] In the reported procedure, Fe_xPt_{1-x} seeds, obtained by simultaneous platinum(II) acetylacetonate reduction and iron carbonyl decomposition, are covered with MFe_2O_4 upon co-decomposition of cobalt and iron acetylacetonate in suitable proportions in the presence of OLAC and OLAM stabilizers. The relevant magnetic data indicate that effective exchange interactions are established between the hard FePt and the soft MFe_2O_4 phases, whose relative proportions dictate the overall coercitivity. Therefore, the chemical engineering of the geometric parameters of these HNCs allows their magnetic properties to be finely tuned for tailored applications.

By using a slight modification of the above-reported procedures for Fe-oxide shell growth, other material combinations have been accessed by seeded techniques.[48,49] For example, biocompatible Me@Fe_2O_3 HNCs (where Me = Co or $SmCo_{5.2}$) have been conjugated by robust dopamine bridging to nitrilotriacetic acid, which possesses high specificity for separating histidine-tagged proteins.[48] $CoFe_2O_4$ NCs have been used as seed substrates to be coated with a Fe_3O_4 layer; however, the product has been demonstrated to be CoFe@Fe_3O_4 HNCs.[49] Although their formation mechanism has not been clarified, this work offers an accurate description of a step-by-step methodology to achieve in-depth structural and compositional information on core@shell nanostructures, which becomes an undoubtedly challenging task when the shell is either polycrystalline or shares an incoherent or lattice-mismatched interface with the core.

3.2 Shell Growth on Molecule-Functionalized Seeds

A number of procedures that involve an intermediate "priming" step have been devised to encapsulate NCs of a variety of materials and metal oxide particles with a SiO_2 or ZrO_2 shell.[49–75] This activation consists of selecting appropriate functional molecules, such as organosilicon or organozirconium compounds that can bind to the surface of NC seeds by means of their functional moiety (e.g., an amine, carboxyl or thiol group) while exposing their alkoxide groups. The latter are hydrolyzed, forming a primary polymerization layer from which a metal oxide network is progressively built upon sequential hydrolysis-condensation reactions with metal alkoxide monomers (Scheme 2, path

b). The procedure for growing a silica shell, on the basis of the so-called Stöber method, has been widely investigated.[63] It consists of three steps, which include surface activation for silanization with a silane coupling agent (such as 3-aminopropyltrimethoxysilane), initial silica deposition with sodium silicate in aqueous solution and extensive growth of the silica shell with a silicon alkoxide, such as tetraethoxysilane, in an alcohol medium. Several improvements and/or simplifications of this general scheme (e.g., by the use of alternative coupling agents, such as polymers or gelatine, or by exploitation of micelle reactors) can be found in the literature.[52–57,61–72] The outer shell surface can itself be provided with additional chemical moieties, serving as a platform for implanting functionalities which would otherwise be hard to anchor onto as-synthesized NCs. Due to the amorphous nature and porous structure which characterize this type of oxide coatings, their deposition does not cause accumulation of significant strain within the global hybrid particle, so that remarkably greater thicknesses can be obtained relative to those normally achievable for crystalline shells. A representative TEM image gallery of core@shell HNCs obtained by this mechanism is displayed in Figure 2.

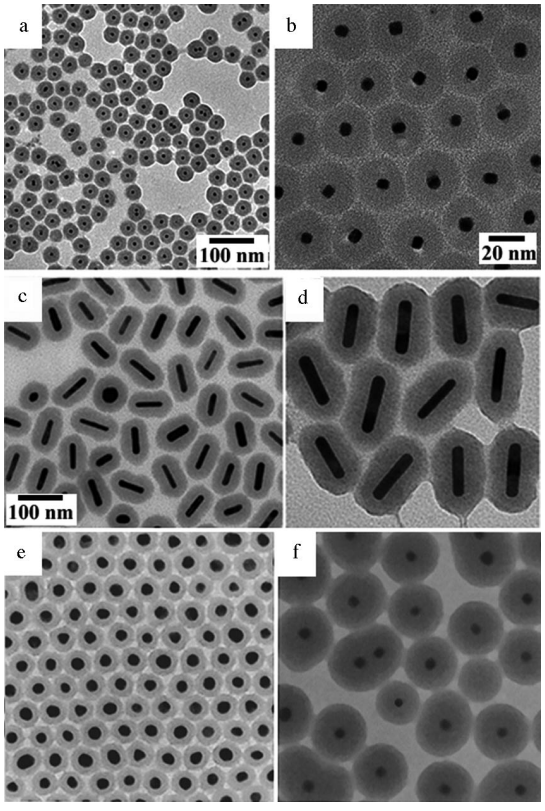

Figure 2. Examples of core@shell HNCs synthesized by chemically activating the surface of seed cores for silica shell growth. Low-magnification transmission electron microscopy (TEM) images of: (a, b) FePt@SiO_2 HNCs (reproduced in part from ref.[70] with permission, copyright 2006 American Chemical Society); (c, d) Au nanorod@SiO_2 HNCs (reproduced in part from ref.[67] with permission, copyright 2006 American Chemical Society); (e, f) Au@SiO_2 HNCs (reproduced in part from ref.[63] with permission, copyright 1996 American Chemical Society).

So far, NC encapsulation with oxides has enabled reaching disparate objectives. Upon SiO_2 coating, high-quality semiconductor NCs (e.g., CdSe, CdSe@ZnS, CdTe, PbSe), which are usually synthesized in organic media and are therefore hydrophobic, have been made soluble and stable in water or buffered solutions, becoming protected against photoinduced degradation while retaining their appealing fluorescence properties.[52–57] Tailoring of the shell surface chemistry has allowed for control of interactions of these NCs with biological environments and their exploitation in optical imaging and/or in the development of detection techniques.[69] Noble metal@SiO_2 HNCs (see, for example, Figure 2c–f) represent another interesting family of functional nanosized building blocks, for which the shell has been added not only to aid dispersion in various media, but also to modify the surface plasmon oscillations of the metal, while guaranteeing their photostability.[62–72] These robust nanostructures provide a contiguous framework for creating a variety of space-filling nanostructures (such as inverse lattices, opals and photonic crystals) and can also act as nanoreactors, whereby reactants can diffuse through the shell, causing modification of the electron density of the cores or its dissolution. These achievements hold clear promise for addressing new catalytic and sensing applications.[57,61,62,65,72]

Magnetic NCs (such as of Fe-oxide, FePt, Co) have been surface-modified with a SiO_2 coating (see, for example, Figure 2a–b), which does not depress their magnetic properties and preserves them from coalescing upon high-temperature processing.[56,68–70,72–74] Moreover, the silica shell effectively prevents toxic heavy metals from being released to the external environment, which is an especially important requirement for these nanomaterials to be practically exploited in biological environments. Consequently, these magnetic@SiO_2 structures, conjugated with suitable receptor molecules, have been proposed as smart platforms that are able to accomplish multiple tasks, such as specific cell targeting and sorting, and imaging.

Complex three-component systems have been recently synthesized by combined approaches.[56,73,74] For example, a reverse microemulsion method has been exploited to synthesize fluorescent, magnetic SiO_2 spheres embodying Fe_3O_4 particles and CdTe quantum dots, whose utility has been demonstrated in immunofluorescence assays.[74] Furthermore, multilayered nanostructures have been fabricated: they consist of a magnetic Fe-oxide core surrounded by a thick silica shell, the latter being further covered with an outer layer of gold. They display strong visible and near-infrared resonance absorption and can be manipulated by using an external magnetic field, two appealing characteristics that hold promise in biomedical applications.[73]

Finally, a case of ZrO_2 coating accomplished by a procedure analogous to that used for silica shell growth processes, is worth mentioning.[75] In the reported work, a priming of Ag NCs with mercaptobenzoic acid has been utilized to enable the subsequent reaction with zirconyl chloride, thereby initiating the formation of a ZrO_2 shell. The resulting Ag@ZrO_2 HNCs can incorporate metal ions

through the permeable oxide, which can be indirectly probed by monitoring the corresponding changes in the surface plasmon resonance of Ag. This finding anticipates a possible use of these materials in ion sensing.

3.3 Shell Formation by Partial Core Oxidation Followed by Vacancy Coalescence

Another viable mechanism towards core@shell structures relies on the sacrificial conversion of the outermost exposed layers of a starting NC core into a different material by a redox replacement reaction (Scheme 2, path c). In this regard, many transition-metal NCs are potentially useful substrates to investigate, since they are easily oxidized when exposed to air, solvated oxygen species or other oxidizing reagents, which leads to the formation of a metal oxide shell at their surface.[76–82] This peculiar reactivity has been largely exploited to create core@shell structures where the mean oxidation state of metal atoms located in the core section is different from that of metal atoms located in the shell section.

It has been found that organic-capped Co NCs exhibit such a high susceptibility to oxidation that a polycrystalline CoO contamination layer can be detected even in samples synthesized by organometallic routes and entirely manipulated under standard air-free techniques. Deliberate and controlled bubbling of oxygen or simple exposure to air of a solution of Co NCs has been used to cause the formation and progressive extension of a CoO shell, until full particle oxidation is eventually obtained.[76,77] Interestingly, the direct communication between the ferromagnetic (FM) Co cubic phase and the antiferromagnetic (AFM) CoO in these Co@CoO HNCs gives rise to the peculiar phenomenon of exchange bias.[76,77,83,84] This effect, observable at temperatures lying between the Néel and the Curie temperature, is due to enhanced unidirectional exchange anisotropy induced by the spin coupling at the FM/AFM interface. It is experimentally manifested by a shift in the hysteresis loops along the direction of the field axis and by a difference in the absolute value of the coercivity with either increasing or decreasing field upon field cooling. In Co@CoO HNCs, exchange bias becomes detectable when a minimum CoO shell thickness is reached, the consequence of which is to enhance the magnetocrystalline anisotropy of Co cores and, in turn, the thermal stability of their magnetic moments. For these reasons, FM/AFM heterostructured systems have been proposed as a potential means to beat the so-called intrinsic "superparamagnetic limit" of nanosized ferromagnets, as well as ideal candidates for high-density magnetic and writing recording media based on spin-valve architectures.[24,85]

Several other types of core@shell HNCs have been similarly obtained by room-temperature air exposure of the respective core seeds. Inverted AFM/ferrimagnetic(FiM) MnO@Mn_3O_4 HNCs have been synthesized by creating a Mn_3O_4 passivating shell on MnO NCs obtained by OLAM-assisted thermal decomposition of manganese acetylacetonate in the presence of an alkanediol under an inert atmosphere.[79] Exchange bias has been verified in these all-oxide heterostructures and systematically quantified as a function of the AFM phase volume in terms of the hysteresis loop shift and the increase in coercivity. This study highlights the fact that the engineering of magnetic anisotropy is indeed possible by means of the AFM/FiM interface in core@shell HNCs by accurately tailoring the size of both core and shell portions in order to achieve the desired magnetic response. Monodisperse crystalline Ni@NiO HNCs[78] and amorphous Fe@Fe-oxide nanoparticles[80] have also been derived from room-temperature oxidation of triphosphane oxide-(TOPO)-capped Ni seeds and OLAM-capped Fe seeds, respectively, which have been provided by established organometallic routes. These superparamagnetic HNCs are potentially appealing in the biomedical field for in-vivo and in-vitro applications such as biomedical separations, magnetic resonance imaging (MRI), contrast enhancement, magnetic-filed-assisted drug delivery and hyperthermal treatment of cancer cells. Promising results in this direction have already been reported for the aforementioned Ni@NiO HNCs, whereby the NiO surface has enabled selective binding of histidine-tagged proteins and their magnetically assisted recovery.[78]

More recently, sophisticated yolk-shell HNCs have been obtained through a mechanism similar to the so-called "Kirkendall effect", an atomic diffusion process that takes place through vacancy exchange rather than by direct interchange of atoms.[86,87] It has been understood that, in a spherical object made of a fast-diffusing core material and an outer layer or reservoir of a slower-diffusing material (e.g., a metal particle that has been surface-passivated with an oxide layer), a net outward transport of matter from the core, and hence a formation of voids, may occur. Under sufficient supply of thermal energy, a huge fraction of the vacancies can ultimately coalesce into a single large void (Scheme 2, path c). This phenomenon has been first verified for reactions of colloidal Co NCs with O_2, sulfur and selenium at moderate temperatures, upon which hollow CoO, CoSe or Co_3S_4 NCs have been formed as the result of a faster outward diffusion of Co cations.[88,89] Refined manipulation of the Kirkendall effect in colloidal systems has led to further increase in topological complexity with the synthesis of Pt@CoO[88] and Fe@Fe_3O_4 yolk-shell[81,82] HNCs in which a void space separates the core from the shell. The former HNCs have indeed been obtained by O_2-driven oxidation of Pt@Co core@shell HNCs in a trioctylphosphane/OLAM/OLAC mixture, in which surface oxidation and vacancy diffusion selectively involves the Co shell portion only. The internal structure of the yolk-shell Pt@CoO HNCs has been additionally assessed by detection of the intact catalytic activity of Pt, confirming that reactants can diffuse through grain boundaries of the CoO shell and reach the surface of the inner metal core.[88] Similar advances toward combined morphological and compositional control have been demonstrated in the temperature-controlled oxidation of monodisperse amorphous Fe nanoparticles by means of either O_2/Ar or trimethylamine *N*-oxide

in octadecene/OLAM solution.[80–82] By these approaches, it has been possible to capture the particle system in different stages of its evolution from the amorphous Fe@Fe-oxide core@shell to the Fe@Fe_3O_4 yolk-shell nanostructures and finally to the crystalline hollow Fe_3O_4 spheres, as illustrated in Figure 3. This findings greatly deepen the understanding of inward/outward diffusion properties that can be induced in colloidal nanoparticles, suggesting useful routes to manipulate them and achieve improved synthesis design.[87]

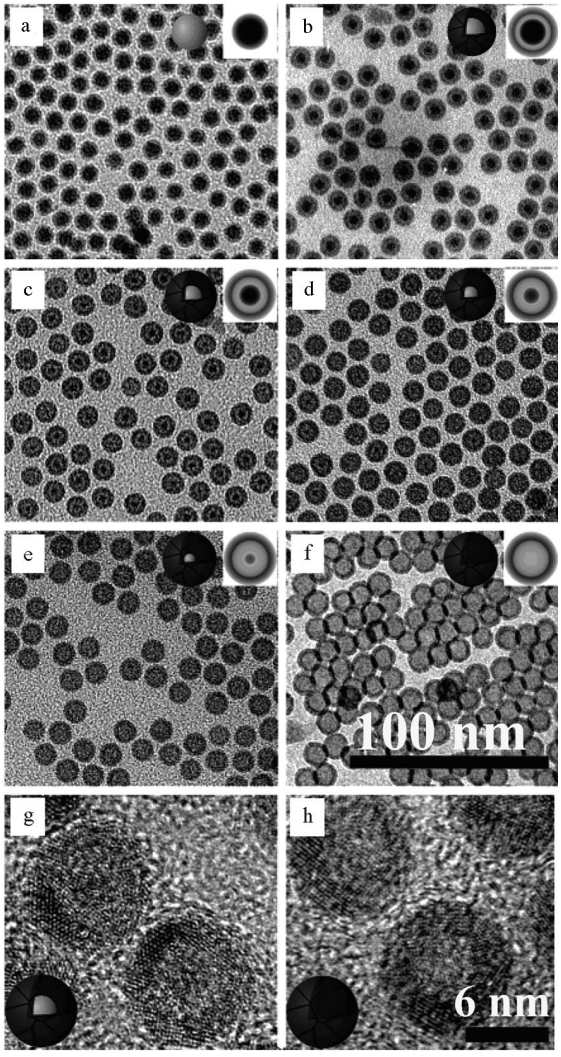

Figure 3. Evolution of core@shell Fe@Fe_3O_4 HNCs by partial oxidation of Fe core seeds followed by vacancy coalescence under exposure to dry 20% oxygen. Low-magnification transmission electron microscopy (TEM) images of the samples grown for: (a) <1 min at room temperature; (b) 1 h at 80 °C; (c) 12 h at 80 °C; (d) 5 min at 150 °C; (e) 1 h at 150 °C; (f) 1 h at 350 °C on a substrate. High-resolution TEM images (g, h) of partially or fully oxidized Fe nanoparticles (reproduced in part from ref.[82] with permission, copyright 2007 American Chemical Society).

3.4 One-Pot Approaches by Self-Controlled Nucleation Growth

There have also been successful efforts to synthesize core@shell HNCs by one-pot approaches, in which all necessary ingredients for material formation are simultaneously present in the same growing solution. The experimental procedure is simplified since no separate seed preparation is required. Appropriate choice of surfactants combined with temperature modulation may set conditions under which the relative reactivities of the material precursors are balanced in such a way that: (a) two different materials are generated separately in time; and (b) the shell material is produced exclusively upon heterogeneous nucleation (Scheme 2, path d). The search for such "smart" colloidal systems, in which the nucleation growth of the core and the shell coating stage are self-regulated, has, however, been extremely challenging up to this date. Actually, only a few cases are available in the literature. For example, metal@oxide HNCs (where Me = Ag or Au, and oxide = TiO_2 or ZrO_2) have been derived by heating a mixture of a titanium or zirconium alkoxide at reflux with the desired noble metal salt in a dimethylformamide/water mixture.[90–93] Thermal activation of dimethylformamide-driven reduction initially leads to a fast in-situ nucleation of metal seeds, which are subsequently passivated by a thin amorphous oxide shell upon slower hydrolysis-condensation reactions of the alkoxide in the presence of a chelating/stabilizing agent. An important property of Ag@TiO_2 HNCs is their ability to accumulate electrons within the Ag core upon TiO_2 photoexcitation, which opens up the possibility of utilizing such charge to affect the metal surface plasmon resonance or to accomplish mild reductive reactions.[92,93]

Another example that better illustrates the concept of the self-controlled nucleation/growth mechanism is provided by the circumstances under which Cr@γ-Fe_2O_3 HNCs are formed.[94] These nanostructures have been synthesized by thermal co-reaction of $Cr(CO)_6$ and $Fe(CO)_5$, which decompose at different rates in mesitylene in the presence of a polymer surfactant. The compositional distribution of the two metal species in the core@shell HNCs has been explained by assuming an initial Fe-cluster-catalyzed formation of the Cr cores, followed by the deposition of a Fe shell and its subsequent oxidation.

4. Noncentrosymmetric Oligomer-Like Architectures

Recently, encouraging advances toward increasingly complex architectures have been made with the development of spatially asymmetric HNCs that embody well-segregated size- and shape-controlled sections of chemically and structurally dissimilar materials into one continuous, all-inorganic hybrid particle. Such nanoheterostructures are distinguished by the fact that the component domains are interconnected by junction regions with limited extension, so that an oligomer-like (nonconcentric) topology is conferred to the overall object. Thus, the elaboration of such types of noncentrosymmetric HNCs is closely analogous to the synthesis of increasingly larger organic molecules bearing a number of functional groups. With respect to the core@shell arrangement, in which only the outer shell sur-

face is chemically accessible, this topological configuration has a twofold advantage. First, it naturally offers multifunctionality, because of the coexistence of the properties inherent to each material unit; and second, it provides a diversified surface platform suitable for implanting a spatially segregated distribution of functional moieties onto a single particle.

In seeded growth syntheses of NCs, several circumstances can concur to bypass the core@shell-type growth regime, leading to HNCs that have a nonconcentric arrangement of their component domains. This will depend on the ultimate surface energy balance accounted for by Equation (1), as discussed earlier. For example, in the attempt to combine materials that are structurally quite uncorrelated, they could tend to minimize the interfacial strain by reducing the contact area between the respective domains with a proportionally smaller cost of additional surface energy.[95,96] On the other hand, a small inorganic junction could form as a means of compensating for the high surface energy values, which would otherwise characterize separate homoparticles of the respective materials, for example, in the case of ineffective organic ligand passivation.[97–100] Other growth conditions leading to noncentrosymmetric HNCs could be determined by the presence of seeds with a pronounced site-specific accessibility, which could arise from differences in the strength of ligand adhesion on the respective facets, in their inherent chemical reactivity or in the specific degree of lattice matching achievable.[43,99–102,115]

4.1 Hetero-Oligomers Based on Spherical Domains

One family of asymmetric HNCs in which oxide materials have been incorporated is represented by heterodimers and hetero-oligomers, comprising two or more nearly spherical NCs of different materials epitaxially attached together. So far, these nanoarchitectures have been synthesized by seeded growth approaches that take advantage of four main mechanisms: (a) direct or surface-activated heterogeneous nucleation; (b) initial nonepitaxial deposition followed by thermal coalescence-crystallization; (c) reaction at liquid/liquid interfaces; and (d) thermally induced attachment of preformed heteroparticles. These pathways are schematically illustrated in Scheme 3a–d. Representative TEM images of such types of HNCs can be found in Figure 4 and Figure 5.

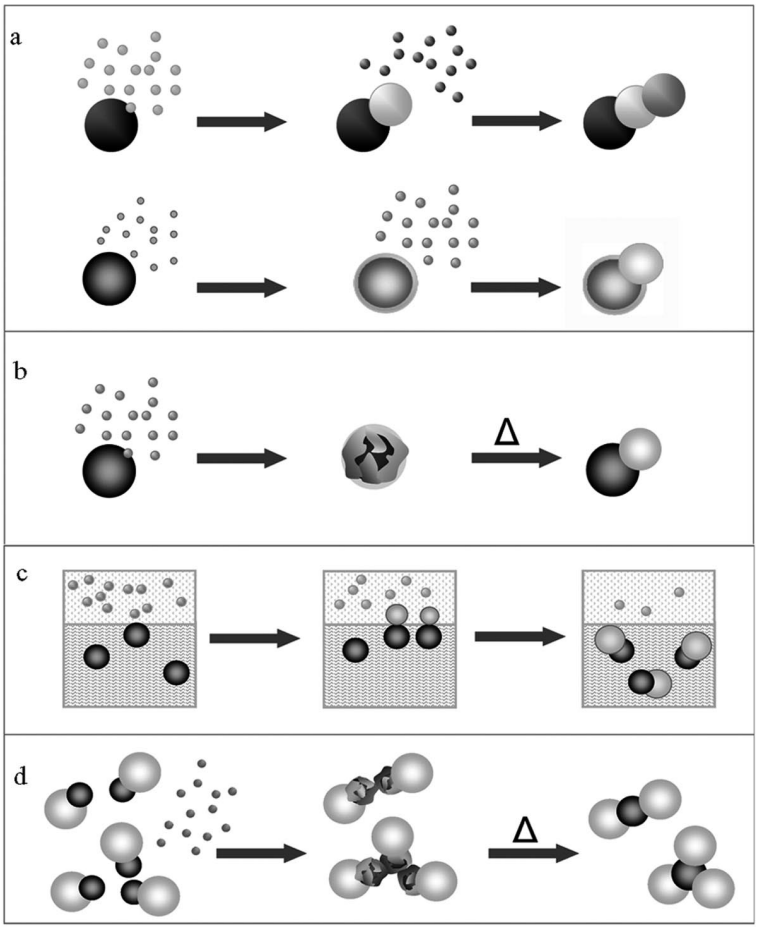

Scheme 3. Sketch of mechanisms leading to the formation of oligomer-type HNCs: (a) direct or surface-activated heterogeneous nucleation onto preformed seeds; (b) initial nonepitaxial deposition followed by thermally induced coalescence-crystallization; (c) reaction at liquid/liquid interfaces; (d) thermally induced attachment of preformed heterodimers.

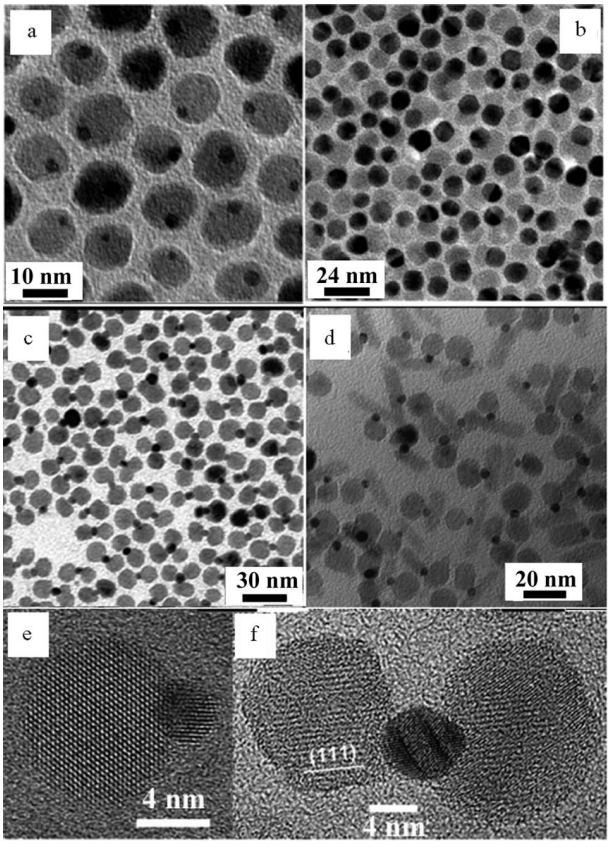

Figure 4. Examples of hetero-oligomer HNCs synthesized by direct epitaxial heterogeneous nucleation (a–b, d, e) and by thermally induced fusion of preformed heterodimers (c, f). Low-magnification transmission electron microscopy (TEM) images of: (a, b) peanut-shaped and dumbbell-like Au–Fe_3O_4 HNCs, respectively (reproduced in part from ref.[101] with permission, copyright 2005 American Chemical Society); (c, d) ternary Fe_3O_4–Au–Fe_3O_4 HNCs and Au–Fe_3O_4–PbS HNCs with a rod-like PbS section (reproduced in part from ref.[43] with permission, copyright 2006 American Chemical Society); (e, f) high-resolution TEM images of Fe_3O_4–Au and Fe_3O_4–Au–Fe_3O_4 HNCs, respectively (reproduced in part from ref.[43] with permission, copyright 2006 American Chemical Society).

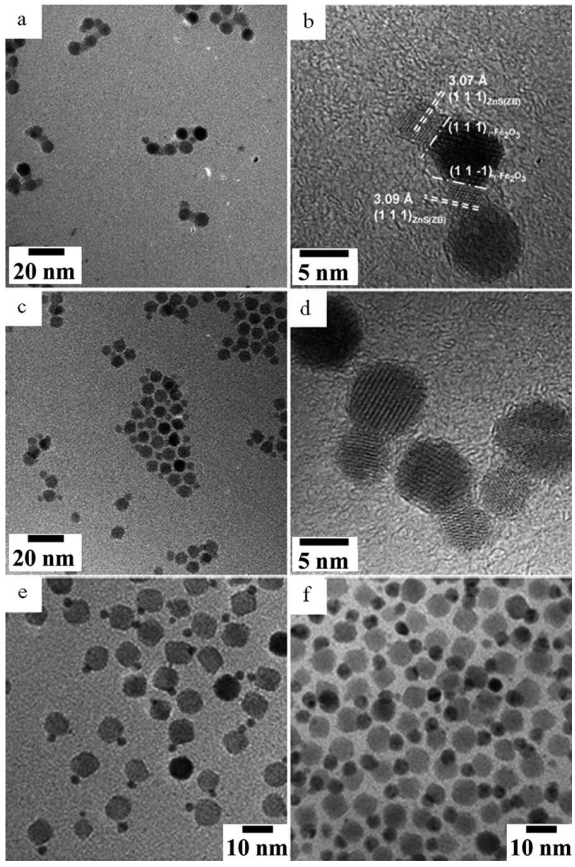

Figure 5. Examples of hetero-oligomer HNCs synthesized by non-epitaxial deposition followed by thermal coalescence-crystallization (a–d), and by reaction at the liquid/liquid interface (e, f). Transmission electron microscopy (TEM) images of: (a, b) Fe_3O_4–ZnS oligomer-like HNCs, (c, d) Fe_3O_4-ZnS dimer HNCs (reproduced in part from ref.[95] with permission, copyright 2005 American Chemical Society) and (e, f) Fe_3O_4–Ag dimer-like HNCs (reproduced in part from ref.[97] with permission, copyright 2005 American Chemical Society).

(a) Direct Epitaxial Heterogeneous Nucleation

Direct heterogeneous nucleation of a second material onto preformed NC seeds in homogeneous solution has been largely exploited in the preparation of HNCs made of various associations of magnetic, metal and semiconductor materials (Scheme 3a, top). HNCs with epitaxially joint Au–Fe_3O_4 or PbS–Fe_3O_4 sections have been synthesized by thermal decomposition of organometallic Fe or Pb/S precursors in the presence of preformed Au NCs in OLAC/OLAM/octadecene mixtures at 200–300 °C.[43,101] Examples are displayed in Figure 4a–b, e. By a conceptually similar scheme, the formation of binary Ag–$CoFe_2O_4$ HNCs has also been claimed by means of Ag deposition onto preformed $CoFe_2O_4$ or PbS nanocrystals in tetralin at mild temperatures; however, the details of the experimental procedure have been elusive.[103] Depending on the relative sizes of the two domains, these heterostructures show a peanut- or dumbbell-like morphological profile. The formation mechanism has been discussed for the case of Au-Fe_3O_4 HNCs.[101] Here the difference in the lattice parameters between the metal and the oxide is likely to be responsible for the dimer-like topology, in which the two domains are then oriented such that they share a coherent interface. In addition, during the synthesis, the solvent plays an important role in regulating the nucleation sites on the Au seeds. In a nonpolar medium, a polarization charge is induced at the Au seed location where Fe_3O_4 is initially grown, which depletes the electron density elsewhere, thus inhibiting further nucleation events. This leads to a dumbbell-like configuration. In contrast, the use of a polar electron-donor solvent allows electron deficiency to be replenished over the Au surface, thus rendering it a suitable ground for the nucleation of multiple Fe_3O_4 domains or even for the achievement of a uniform oxide coverage. Thus, either flower-like heterostructures, made of several Fe_3O_4 "petals" arranged on a central Au particle, or Au@Fe_3O_4 core@shell HNCs have been obtained, depending on the specific solvent and on the temperature used.[101] These findings clearly highlight how

decisive the impact of changes in the solution environment is on the setting of the overall surface energy balance and, in turn, on the final topology of the resulting HNCs.

A more general approach to the fabrication of dumbbell-like HNCs based on previous synthetic knowledge and comprising one noble metal domain and a section of a magnetic or semiconductor material has been patented.[104] This strategy relies on performing a preliminary surface "activation" of the seeds by depositing a layer of elemental S, Se, metal sulfide or metal selenide onto their surface. Such treatment facilitates subsequent heterogeneous growth of an additional material domain from the respective molecular precursors (Scheme 3a, bottom). Different classes of heterodimers can be synthesized, including magnetic metals and metal oxides (e.g., Co, Ni, Fe, Fe_3O_4, $CoFe_2O_4$, $MnFe_2O_4$, $NiFe_2O_4$) associated with Ag and Au or semiconductors (e.g., PbSe, PbS, CdSe, CdS) combined with Au, Ag, Pt or Pd. Again, the remarkable structural difference between the materials that are brought together can explain the formation of the heterodimer topology.

An even higher architectural complexity has been reached by applying reiterated seeding steps, as a means of increasing the number of component domains in a NC-based heterostructure (Scheme 3a, top). As a remarkable demonstration of this concept, ternary Fe_3O_4–Au–PbSe (or Fe_3O_4–Au–PbS) hetero-oligomer HNCs have been achieved by inducing heterogeneous nucleation of PbSe (or PbS) on Fe_3O_4–Au dumbbell-shaped seeds from Pb/Se (or Pb/S) surfactant complexes (an example is shown in Figure 4d).[43] In addition, it has been shown that a mechanism resembling the solution-liquid-solid growth of nanowires from metal seed catalysts is responsible for the formation of various anisotropically shaped PbSe nanostructures, which initially depart out of the Fe_3O_4–Au seeds and then detach from them.[105] An example is reported in Figure 4d. The properties of these magnetic-metal-semiconductor HNCs deviate from those of the individual components alone. For example, the semiconductor luminescence is quenched as a result of electron migration toward the metal domain, while the plasmon resonance is largely red-shifted due to dielectric coating effects. Also, the relevant magnetic parameters are altered; however, a straightforward explanation for these changes has not been reported yet.[43,101]

More recently, luminescent ZnO–Au heterodimers have been obtained by a room-temperature aqueous route.[98] Here, the presence of weakly acetate-passivated facets on ZnO NC seeds is essential to aid epitaxial Au deposition upon citrate-induced gold ion reduction under such mild reaction conditions. These ZnO–Au HNCs exhibit red-shifted Au surface plasmon absorption and ZnO band-edge UV emission that is about one order of magnitude more intense than that of pure ZnO NCs. Also, multiphonon Raman scattering is enhanced by the strongly localized electromagnetic field of the metal plasmon, as observed in other types of composite systems.[106,107] These modified properties again reflect the mutual influence of interfacial electron communication that is achieved upon formation of a inorganic heterojunction.

(b) Nonepitaxial Deposition and Thermal Coalescence Crystallization

A systematic investigation of how minimization of interfacial strain energy governs the topological evolution of HNCs has been reported for heterostructures based on γ-Fe_2O_3 and a MeS (where Me = Cd, Zn, Hg) compound.[95,96] The synthesis of these HNCs is seeded with γ-Fe_2O_3 NCs, onto which a highly defective and amorphous MeS layer is initially deposited upon sequential addition of metal acetate and sulfur precursors at low temperature (lower than 100 °C). Upon thermal annealing at 280 °C, the amorphous MeS shell starts to crystallize, which determines a gradual strain intensification at the γ-Fe_2O_3/MeS junction region owing to the poor lattice matching between the two materials. Over time, the shell coalesces and segregates into a discrete MeS grain, which is ultimately attached at one side to the original seed (Scheme 3b). Such evolution can be explained by considering that the large junction tension in the initial γ-Fe_2O_3@MeS core@shell nanostructure can be greatly relieved if the interfacial area is reduced. This process fully compensates for the increase in the overall surface energy that eventually accompanies heterodimer formation. The topological evolution of the γ-Fe_2O_3–MeS system has been studied as a function of the MeS type and rationalized on the basis of the Coincidence Site Lattice Theory.[108] It has been proposed that, since the lattice fit at a γ-Fe_2O_3/MeS interface is better for Me = Zn than for Me = Cd and much worse for Me = Hg, then the heterogeneous growth of MeS on γ-Fe_2O_3 NPs could lead to multiple ZnS domains or to only one CdS domain on each oxide seed, while the formation of γ-Fe_2O_3–HgS heterodimers should be quite unfavourable. Examples of HNCs synthesized by this mechanism are reported in Figure 5a–d.

As for their chemical-physical properties, these γ-Fe_2O_3–MeS HNCs retain both the fluorescence of the MeS domain and the typical superparamagnetic behaviour of iron oxide, and they could therefore be conveniently used as bifunctional probes, for instance, in the biomedical field. First efforts in this direction have been recently made with the γ-Fe_2O_3–CdSe heterodimer counterparts (synthesized by a similar approach) of these HNCs, which were silica-coated and bioconjugated in order to be used in the imaging of live cell membranes.[56]

(c) Biphasic Reactions

An original route for synthesizing heterodimers comprising a Fe-oxide section and either a Au or a Ag domain under mild conditions has been based on seeded growth at a liquid/liquid interface.[97] In the reported procedure (Scheme 3c), an aqueous metal salt solution is brought in contact with an organic solvent immiscible with the aqueous solution (such as dichlorobenzene, dichloromethane, hexane or octyl ether) in which surfactant-capped Fe_3O_4 NCs are dissolved. Upon ultrasonic irradiation under an oxygen-free atmosphere, an emulsion is formed and stabilized by the hydrophobic Fe_3O_4 seeds that self-assemble at the organic/water interfaces of the microdroplets.[97] The

oxide NCs provide catalytic sites on which the Ag^+ or $AuCl_4^-$ ions can be reduced to Ag or Au, respectively, by sonochemically produced radicals. As the Fe_3O_4 seeds are only partially exposed to the aqueous phase, metal deposition is confined to a small surface region and proceeds self-catalytically, which explains why a single metal domain is ultimately found on each Fe_3O_4. The final HNCs are fully soluble in the nonaqueous phase. This route has been extended also to the preparation of Fe_3O_4–Au, FePt–Ag and Au–Ag heterodimers. An appealing characteristic of these hybrid nanostructures is that they offer two material platforms with substantially different surface properties. As a proof of concept, it has been indeed possible to selectively functionalize each one of the two domains with different biomolecules. Examples of HNCs synthesized by this biphasic strategy are shown in Figure 5e, f.

(d) Reactions between HNCs

An original strategy has been devised with the potential to access increasingly complex HNCs. It has been reported[43] that peanut-shaped ternary Fe_3O_4–Au–Fe_3O_4 HNCs, in which an Au section bridges two Fe_3O_4 domains, can be obtained by inducing the coalescence of the Au domains that belong to separate Au–Fe_3O_4 heterodimers in the presence of sulfur (Scheme 3d). Thus, in this approach, heterodimers are regarded as small functional molecules that can be combined with each other to form larger molecules. With its high affinity for gold surfaces, it may be presumed that sulfur helps to displace the capping surfactants on the Au section of the heterodimers, thereby driving them to lower their surface energy by fusing with each other. An example of the as-synthesized HNCs is reported in Figure 4c, f.

4.2 Asymmetric Heterostructures Based on Rod-Shaped Oxide Sections

HNCs with an even more pronounced asymmetry in the spatial distribution of their component domains have been obtained by controlling heterogeneous growth reactions on nonspherical oxide NCs, such as ZnO or TiO_2 nanorods. NCs with such shapes commonly occur in highly asymmetric crystalline phases (e.g., the hexagonal wurtzite for ZnO and the tetragonal anatase for TiO_2), exhibiting a preferential elongation along the direction of their *c* axes. An important aspect to emphasize is that the chemical reactivity of the basal planes of nanorods can differ significantly from that of their longitudinal sidewalls, which is consistent with the anisotropic growth mechanism by which they are obtained.[111,112] Variations in the strength of surface ligand binding and/or in the degree of interfacial strain at the relevant junction regions can lead to site-selective nucleation of a different material on these nanorods when they are used as seeds. Nevertheless, accurate control over the final HNC topology has proven to be inherently difficult, which explains why progress in this area is still in its infancy.

Two types of HNCs based on ZnO nanorods have been reported, both of which can be expected to exhibit enhanced charge-carrier-separating properties relevant to photocatalytic and photovoltaic applications.[110,115] A light-assisted method has been developed for preparing Ag-functionalized ZnO nanorods.[100] Their growth has been based on the UV-induced photocatalytic reduction of silver ions on acetate-capped ZnO nanorods prepared by oriented attachment of isotropic particles formed upon controlled hydrolysis of zinc acetate.[111] Upon ZnO bandgap photoexcitation, electron-hole pairs are generated, which are then available to react with suitable acceptors at the oxide surface. Because of the weak organic passivation on the seed facets, metallic Ag embryos can easily be deposited at room temperature and self-catalyze their subsequent enlargement, which prevails over additional nucleation. A preferential deposition of Ag domains in the proximity of either one of the nanorod tips has been observed and tentatively explained as arising from internal-dipole-driven localization of conduction electrons on those regions and/or from more favourable lattice match conditions for the respective material lattices. In another report, the tip-preferential deposition of TiO_2 onto similar acetate-capped ZnO nanorods has been observed.[115] In this case, the hydrothermal treatment of the ZnO nanorods with amorphous TiO_2 powders has been manipulated to synthesize heterostructures, each comprising one amorphous TiO_2 head cap attached to either one of the nanorod tips. The latter have been identified to coincide with the polar basal planes of *c*-axis-elongated wurtzite lattices and tentatively considered as more chemically reactive because of their inherent structure.[115]

Semiconductor–magnetic heterostructures based on anisotropic TiO_2 portions have been successfully synthesized by suitable manipulation of the organometallic chemistry in complex surfactant mixtures. One remarkable example of strain-driven heteroepitaxial growth is represented by the synthesis of asymmetric binary HNCs, each made of one rod-like anatase TiO_2 section and one γ-Fe_2O_3 spherical domain attached together,[102] which are shown in Figure 6. These heterostructures have been obtained by accomplishing $Fe(CO)_5$ decomposition at 240–300 °C in an octadecene solution containing hydrolytically prepared TiO_2 nanorods[112] and three surfactants, namely OLAC, OLAM and 1,2-hexadecandiol, in defined relative proportions. The proposed synthetic approach demonstrates to be highly versatile in that it allows to finely tailor the mean dimensions of the γ-Fe_2O_3 that are heterogeneously nucleated on the TiO_2 seeds by adjusting the reaction parameters. The γ-Fe_2O_3 size-tuning has been rationalized in terms of the competition between homogeneous and heterogeneous nucleation processes and on the basis of the balance attained between the nucleation and growth stages. Temperature influences the exchange dynamics between the surfactants bound to the seed surface and the free ligands in the solution, hence dictating the number of TiO_2 nanorods that become activated for γ-Fe_2O_3 deposition. Simultaneously, the TiO_2-to-$Fe(CO)_5$-precursor ratio regulates the availability of monomers that can feed the growth of the Fe-oxide nucleated

heterogeneously. From the structural point of view, the most striking feature of these HNCs is that the γ-Fe_2O_3 domain grows exclusively on the longitudinal sides of the TiO_2 nanorod seeds. As a result of the high lattice misfit that characterizes the relevant γ-Fe_2O_3/TiO_2 junction planes, the TiO_2 section is deformed and bowed toward the γ-Fe_2O_3 sphere. Detailed structural analyses have indeed disclosed the involvement of a peculiar heteroepitaxial growth mechanism that is typically encountered during MBE growth of quantum dot islands on highly mismatched substrates.[113,114] According to the latter, the TiO_2 and γ-Fe_2O_3 domains are coherently connected by a rather limited junction area at which the near-surface planes of the respective materials are locally curved, as sketched in Scheme 4a. This allows the strain accumulated at the interface to be accommodated to a great extent, only at a proportionally smaller cost of additional surface energy.[113,114] The possibility of tuning the dimensions of the iron oxide section translates into a fine control over the magnetic properties of the HNCs, which closely resemble those of free γ-Fe_2O_3 particles, as a result of the limited contact area shared with TiO_2.

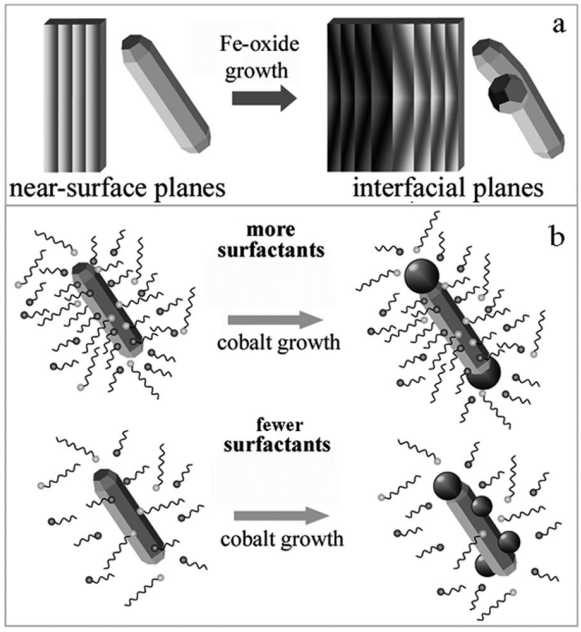

Scheme 4. Sketch of mechanisms leading to the formation of asymmetric HNCs based on anisotropically shaped TiO_2 sections: (a) γ-Fe_2O_3–TiO_2 epitaxial junctions achieved by local curving of interfacial planes; (b) surfactant-controlled site-selective heterogeneous growth of ε-Co onto TiO_2 nanorod seeds.

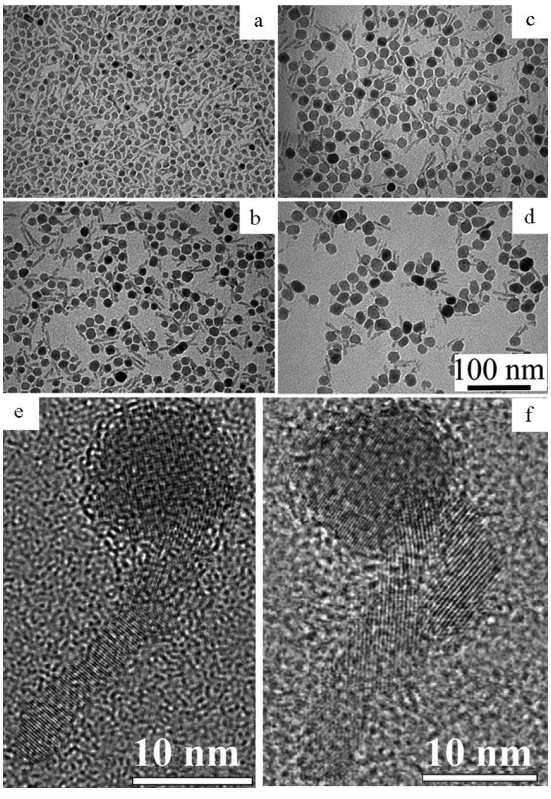

Figure 6. Examples of asymmetric HNCs synthesized by heterogeneous growth of γ-Fe_2O_3 spherical domains onto TiO_2 nanorods. (a–d) Low-magnification transmission electron microscopy (TEM) images of γ-Fe_2O_3–TiO_2 HNCs with increasingly larger γ-Fe_2O_3 spheres. (e) High-resolution TEM image of a γ-Fe_2O_3–TiO_2 matchstick-shaped HNC made of a TiO_2 nanorod connected to a γ-Fe_2O_3 spherical head. (f) High-resolution TEM image of a γ-Fe_2O_3–TiO_2 heterostructure, comprising a fork-shaped TiO_2 nanorod attached to γ-Fe_2O_3 sphere by its arms (reproduced in part from ref.[102] with permission, copyright 2006 American Chemical Society).

By a TiO_2 seeded growth strategy similar to that described above, site-selectively ε-Co-decorated TiO_2 nanorods have been synthesized by thermal decomposition of $Co_2(CO)_8$ with the assistance of octanoic acid (OCAC), OLAM and OLAC at 250–280 °C.[99] A calibrated temporal variation of the surfactant composition and/or concentration along the synthesis course has been conveniently used to switch the manner of heterogeneous Co growth from a tip-preferential mode to a nonselective deposition regime, in which the metal also nucleates onto the longitudinal sidewalls of the NRs. Such a degree of control is illustrated in Figure 7. According to an in-depth atomic-resolution structural investigation, both types of TiO_2–Co heterojunction configuration are quite favourable in terms of lattice point coincidence, which therefore excludes the possibility that the site-selective Co deposition is dominantly driven by facet-dependent interfacial strain. Instead, a major role in achieving the topological control is played by the surfactants here. They not only regulate the TiO_2 seed accessibility, adsorbing in a facet-selective manner, but also stabilize the growing Co domains, as sketched in Scheme 4b. It has been rationalized that the attainment of a TiO_2–Co junction becomes favoured when it compensates for the increase in the overall surface tension caused by inadequate surface passivation by the ligands. Notably, the magnetic properties of these TiO_2–Co HNCs do not follow a simple dependence on the Co domain size. One possible explanation could be that, as the two materials communicate

through a rather extended inorganic junction, proximity effects and/or exchange bias at the interface can have an unusual influence on the magnetic anisotropy term.[99]

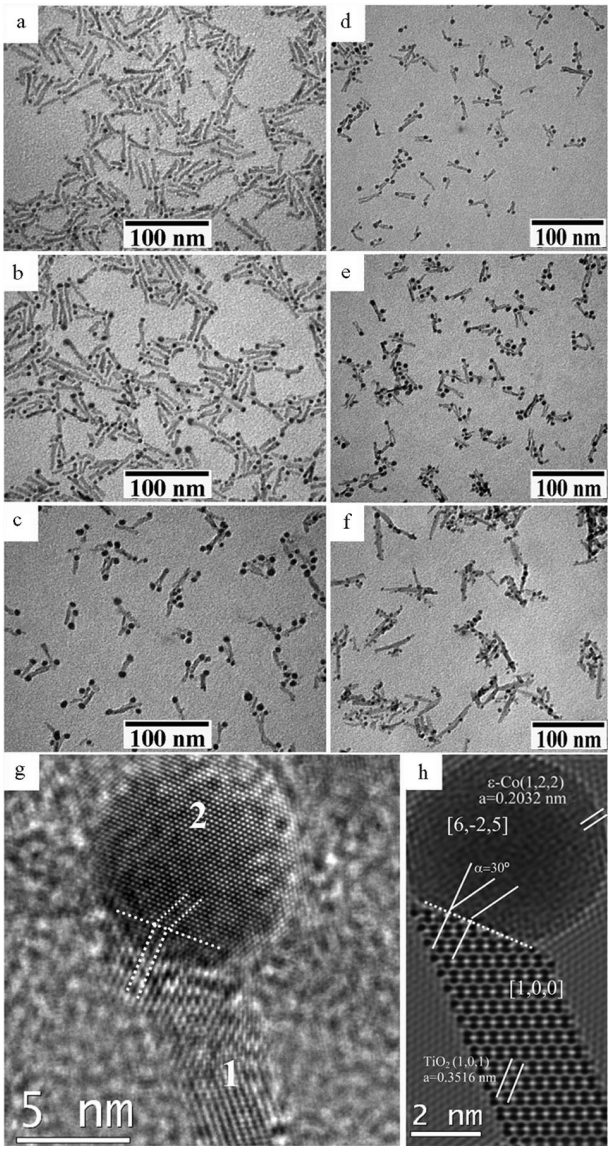

Figure 7. Examples of asymmetric hybrid nanocrystals (HNCs) synthesized by heterogeneous growth of ε-Co spherical domains onto TiO_2 nanorods. Low-magnification transmission electron microscopy (TEM) images of Co-tipped TiO_2 nanorod HNCs with tuneable Co tip size (a–c) and of longitudinally Co-decorated TiO_2 nanorod HNCs (d–f). In (g) and (h), a high-resolution TEM image of a Co–TiO_2 matchstick-like HNC and its corresponding simulated image, onto which the relevant epitaxial relationships are marked, are reported, respectively (reproduced in part from ref.[99] with permission, copyright 2007 American Chemical Society).

It is believed that these asymmetric oxide-based NCs could give rise to disparate technological applications. Indeed, these objects represent nanosized bifunctional catalysts for a variety of gas- and liquid-phase reactions. An appealing aspect of the heterostructures is that the photocatalytic activity of TiO_2 is combined with the magnetism of γ-Fe_2O_3 or of Co, that could enable fluidization, production of local heating in the solution, as well as catalyst recovery upon application of an external magnetic field. Exciting applications in the biomedical field can also be envisioned. The nontoxic γ-Fe_2O_3 domain could be used to drive the HNCs toward tumour tissues, where magnetically induced hyperthermia could be combined with TiO_2-based photodynamic therapy to kill malignant cells. Finally, it could be possible to deliberately orient TiO_2 nanorods anchored onto surfaces under an external field, which would open up novel perspectives in the controlled organization of multifunctional nanocrystals on substrates.

5. Concluding Remarks

The synthesis of multimaterial hybrid nanocrystals based on combined sections of oxide, metal and semiconductor materials is attracting increasing attention as a new fascinating branch of nanochemistry research. The preparation of NC heterostructures is a rather challenging task, as the ability to tailor specific nanosized materials must be integrated with an understanding of the parameters which determine heterogeneous and/or heteroepitaxial growth at the nanoscale level. At present, these nanocrystal-based structures cannot yet be engineered in such a way as to prevent possible detrimental effects on the properties of individual material components. Nevertheless, the possibility to design and synthesize elaborate HNCs with a topologically controlled composition promises to disclose unprecedented horizons in the manipulation of the properties of any nanosized metal, semiconductor and oxide material that is brought into contact with other materials. It can be expected that future progress in this synthetic ability will open up access to new breeds of colloidal nanoheterostructures, which could enable optoelectronic, magnetic, biomedical, photovoltaic and catalytic applications with a high level of performance.

Acknowledgments

This work was partially supported by the Italian project FIRB (Contract No. RBLA03ER38).

[1] Y. Yin, A. P. Alivisatos, *Nature* **2005**, *437*, 664–670.
[2] C. Burda, X. B. Chen, R. Narayanan, M. A. El-Sayed, *Chem. Rev.* **2005**, *105*, 1025–1102.
[3] Y.-w. Jun, J.-s. Choi, J. Cheon, *Angew. Chem. Int. Ed.* **2006**, *45*, 3414–3439.
[4] P. D. Cozzoli, T. Pellegrino, L. Manna, *Chem. Soc. Rev.* **2006**, *35*, 1195–1208.
[5] J. Park, J. Joo, S. G. Kwon, Y. Jang, T. Hyeon, *Angew. Chem. Int. Ed.* **2007**, *46*, 4630–4660.
[6] M. Fernández-García, A. Martinez-Arías, J. C. Hanson, J. A. Rodríguez, *Chem. Rev.* **2004**, *104*, 4063–4104.
[7] J. A. Rodríguez, Fernández-García, *Synthesis Properties, and Applications of Oxide Nanomaterials*, John Wiley & Sons, Inc., Hoboken, New Jersey, **2007**, 717 pp.
[8] J. Reed, G. Ceder, *Chem. Rev.* **2004**, *104*, 4513–4534.
[9] M. Chiesa, M. C. Paganini, E. Giamello, D. M. Murphy, C. Di Valentin, G. Pacchioni, *Acc. Chem. Res.* **2006**, *39*, 861–867.
[10] J. Zhao, B. Li, K. Onda, M. Feng, H. Petek, *Chem. Rev.* **2006**, *106*, 4402–4427.

[11] R. Osgood, *Chem. Rev.* **2006**, *106*, 4379–4401.
[12] M. Niederberger, *Acc. Chem. Res.* **2007**, *40*, 793–800.
[13] S. B. Adler, *Chem. Rev.* **2004**, *104*, 4791–4843.
[14] S. McIntosh, R. J. Gorte, *Chem. Rev.* **2004**, *104*, 4845–4865.
[15] X. Chen, S. S. Mao, *Chem. Rev.* **2007**, *107*, 2891–2959.
[16] Y.-w. Jun, Y.-M. Huh, J.-s. Choi, J.-H. Lee, H.-T. Song, S.-j. Kim, S. Yoon, K.-S. Kim, J.-S. Shin, J.-S. Suh, J. Cheon, *J. Am. Chem. Soc.* **2005**, *127*, 5732–5733.
[17] Y.-w. Jun, J.-t. Jang, J. Cheon, *Bull. Korean Chem. Soc.* **2006**, *27*, 961–971.
[18] S. Kudera, L. Carbone, E. Carlino, R. Cingolani, P. D. Cozzoli, L. Manna, *Physica E* **2007**, *37*, 128–133.
[19] J. W. Mullin, *Crystallization*, 3rd ed, Butterworth-Heinemann, Oxford, **1997**.
[20] T. Sugimoto, *Monodisperse Particles*, Elsevier, Amsterdam, **2001**.
[21] I. V. Markov, *Crystal Growth for Beginners: Fundamentals of Nucleation, Crystal Growth, and Epitaxy*, World Scientific, Singapore, **2003**.
[22] I. Markov, *Mater. Chem. Phys.* **1997**, *49*, 93–104.
[23] A. Y. Cho, *J. Cryst. Growth* **1999**, *202*, 1–7.
[24] K. Li, Y. Wu, Z. Guo, Y. Zheng, G. Han, J. Qiu, P. Lu, L. An, T. Zhou, *J. Nanosci. Nanotechnol.* **2007**, *7*, 13–45.
[25] H. Sakai, K. N. Yu, H. Shibata, T. Ohkubo, M. Abe, *J. Am. Chem. Soc.* **2006**, *128*, 4944–4945.
[26] G. Oldfield, T. Ung, P. Mulvaney, *Adv. Mater.* **2000**, *12*, 1519–1522.
[27] J. Li, H. C. Zeng, *Angew. Chem. Int. Ed.* **2005**, *44*, 4342–4345.
[28] P. Mulvaney, M. Giersing, T. Ung, L. M. Liz-Marzán, *Adv. Mater.* **1997**, *9*, 570–575.
[29] A. S. Nair, T. T. Renys, V. Suryanarayanan, T. Pradeep, *J. Mater. Chem.* **2003**, *13*, 297–300.
[30] D. S. Koktysh, X. Liang, B.-G. Yun, I. Pastoriza-Santos, R. L. Matts, M. Giersig, C. Serra-Rodríguez, L. M. Liz-Marzán, N. A. Kotov, *Adv. Funct. Mater.* **2002**, *12*, 255–265.
[31] V. W. Subramanian, E. E. Wolf, P. V. Kamat, *J. Phys. Chem., B* **2003**, *107*, 7479–7485.
[32] V. W. Subramanian, E. E. Wolf, P. V. Kamat, *Langmuir* **2003**, *19*, 469–474.
[33] A. Dawson, P. V. Kamat, *J. Phys. Chem., B* **2001**, *105*, 960–966.
[34] P. V. Kamat, M. Flumiani, A. Dawson, *Colloid Surf. A* **2002**, *202*, 269–279.
[35] A. Wood, M. Giersig, P. Mulvaney, *J. Phys. Chem., B* **2001**, *105*, 8810–8815.
[36] T. Hikov, M.-K. Schroeter, L. Khodeir, A. Chemseddine, M. Muhler, R. A. Fischer, *Phys. Chem. Chem. Phys.* **2006**, *8*, 1550–1555.
[37] T. Gao, Q. Li, T. Wang, *Chem. Mater.* **2005**, *17*, 887–892.
[38] G. Shan, X. Kong, X. Wang, Y. Liu, *Surf. Sci.* **2005**, *582*, 61–68.
[39] L. Y. Wang, J. Luo, Q. Fan, M. Suzuki, I. S. Suzuki, M. H. Engelhard, Y. H. Lin, N. Kim, J. Q. Wang, C. J. Zhong, *J. Phys. Chem., B* **2005**, *109*, 21593–21601.
[40] H.-Y. Park, M. J. Schadt, L. Wang, I.-I. S. Lim, P. N. Njoki, S. H. Kim, M.-Y. Jang, J. Luo, C.-J. Zhong, *Langmuir* **2007**, *23*, 9050–9056.
[41] J. L. Lyon, D. A. Fleming, M. B. Stone, P. Schiffer, M. E. Williams, *Nano Lett.* **2004**, *4*, 719–723.
[42] P. Gong, H. Li, X. He, K. Wang, J. Hu, W. Tan, S. Zhang, X. Yang, *Nanotechnology* **2007**, *18*, 285604–285610.
[43] W. Shi, H. Zeng, Y. Sahoo, T. Y. Ohulchanskyy, Y. Ding, Z. L. Wang, M. Swihart, P. N. Prasad, *Nano Lett.* **2006**, *6*, 875–881.
[44] X. Teng, D. Black, N. J. Watkins, Y. L. Gao, H. Yang, *Nano Lett.* **2003**, *3*, 261–264.
[45] H. Yang, X. Teng, *Nanotechnology* **2005**, *16*, S554–S561.
[46] H. Zeng, J. Li, Z. L. Wang, J. P. Liu, S. H. Sun, *Nano Lett.* **2004**, *4*, 187–190.
[47] H. Zeng, S. H. Sun, J. Li, Z. L. Wang, J. P. Liu, *Appl. Phys. Lett.* **2004**, *85*, 792–794.
[48] C. Xu, K. Xu, H. Gu, R. Zheng, H. Liu, X. Zhang, Z. Guo, B. Xu, *J. Am. Chem. Soc.* **2004**, *126*, 9938–9939.
[49] J. Li, H. Zheng, S. Sun, J. P. Liu, Z. L. Wang, *J. Phys. Chem., B* **2004**, *108*, 14005–14008.
[50] P. Mulvaney, L. M. Liz-Marzan, M. Giersig, T. Ung, *J. Mater. Chem.* **2000**, *10*, 1259–1270.
[51] D. Gerion, F. Pinaud, S. C. Williams, W. J. Parak, D. Zanchet, S. Weiss, A. P. Alivisatos, *J. Phys. Chem., B* **2001**, *105*, 8861–8871.
[52] M. A. Correa-Duarte, M. Giersig, L. M. Liz-Marzan, *Chem. Phys. Lett.* **1998**, *286*, 497–501.
[53] M. Bruchez, M. Moronne, P. Gin, S. Weiss, A. P. Alivisatos, *Science* **1998**, *281*, 2013–2016.
[54] Y. Wang, Z. Thang, X. Liang, L. M. Liz-Marzan, N. A. Kotov, *Nano Lett.* **2004**, *4*, 225–231.
[55] Z. Zhelev, H. Ohba, R. Bakalova, *J. Am. Chem. Soc.* **2006**, *128*, 6324–6325.
[56] S. T. Selvan, P. K. Patra, C. Y. Ang, J. Y. Ying, *Angew. Chem. Int. Ed.* **2007**, *46*, 2448–2452.
[57] A. Burns, H. Ow, U. Wiesner, *Chem. Soc. Rev.* **2006**, *35*, 1028–1042.
[58] A. Wolcott, D. Gerion, M. Visconte, J. Sun, A. Schwartzberg, S. Chen, J. Z. Zhang, *J. Phys. Chem., B* **2006**, *110*, 5779–5789.
[59] M. Darbandi, W. Lu, J. Fang, T. Nann, *Langmuir* **2006**, *22*, 4371–4375.
[60] S. H. Liu, M. Han, *Adv. Funct. Mater.* **2005**, *15*, 961–967.
[61] T. Ung, L. M. Liz-Marzan, P. Mulvaney, *J. Phys. Chem., B* **1999**, *103*, 6770–6773.
[62] L. M. Liz-Marzan, *Langmuir* **2006**, *22*, 32–41.
[63] L. M. Liz-Marzan, M. Giersing, P. Mulvaney, *Langmuir* **1996**, *12*, 4329–4335.
[64] T. Ung, L. M. Liz-Marzan, P. Mulvaney, *Langmuir* **1998**, *14*, 3740–3748.
[65] V. Salgueirino-Maceira, F. Caruso, L. M. Liz-Marzan, *J. Phys. Chem., B* **2003**, *107*, 10990–10994.
[66] Y. Kobayashi, H. Katakami, E. Mine, D. Nagao, M. Konno, L. M. Liz-Marzan, *Colloid Interface Sci.* **2005**, *283*, 392–396.
[67] I. Pastoriza-Santos, J. Perez-Juste, L. M. Liz-Marzan, *Chem. Mater.* **2006**, *18*, 2465–2467.
[68] Y. Kobayashi, M. Horie, M. Konno, B. Rodriguez-Gonzalez, L. M. Liz-Marzan, *J. Phys. Chem., B* **2003**, *107*, 7420–7425.
[69] T.-J. Yoon, K. N. Yu, E. Kim, J. S. Kim, B. G. Kim, S.-H. Yun, B.-H. Sohn, M.-H. Cho, J.-K. Lee, S. B. Park, *Small* **2006**, *2*, 209–215.
[70] D. C. Lee, F. V. Mikulec, J. M. Pelaez, B. Koo, B. A. Korgel, *J. Phys. Chem., B* **2006**, *110*, 11160–11166.
[71] T. Ung, L. M. Liz-Marzan, P. Mulvaney, *J. Phys. Chem., B* **2001**, *105*, 3441–3452.
[72] L. M. Liz-Marzan, P. Mulvaney, *J. Phys. Chem., B* **2003**, *107*, 7312–7326.
[73] V. Salgueirino-Maceira, M. A. Correa-Duerte, M. Farle, A. Lopez-Quintela, K. Sieradzki, R. Diaz, *Chem. Mater.* **2006**, *18*, 2701–2706.
[74] R. He, X. You, J. Shao, F. Gao, B. Pan, D. Cui, *Nanotechnology* **2007**, *18*, 315601.
[75] V. Eswaranand, T. Pradeep, *J. Mater. Chem.* **2002**, *12*, 2421–2425.
[76] J. B. Tracy, D. N. Weiss, D. P. Dinega, M. G. Bawendi, *Phys. Rev. B* **2005**, *72*, 064404, 1–8.
[77] M. Verelst, T. O. Ely, C. Amiens, E. Snoeck, P. Lecante, A. Mosset, M. Respaud, J. M. Broto, B. Chaudret, *Chem. Mater.* **1999**, *11*, 2702–2708.
[78] I. S. Lee, N. Lee, J. Park, B. H. Kim, Y.-W. Yi, T. Kim, T. K. Kim, I. H. Lee, S. R. Paik, T. Hyeon, *J. Am. Chem. Soc.* **2006**, *128*, 10658–10659.
[79] G. Salazar-Alvarez, J. Sort, S. Suriñach, M. D. Baró, J. Nogués, *J. Am. Chem. Soc.* **2007**, *129*, 9102–9108.
[80] S. Peng, C. Wang, J. Xie, S. Sun, *J. Am. Chem. Soc.* **2006**, *128*, 10676–10677.
[81] S. Peng, S. Sun, *Angew. Chem. Int. Ed.* **2007**, *46*, 4155–4158.

[82] A. Cabot, V. F. Puntes, E. Shevchenko, Y. Yin, L. Balcells, M. A. Marcus, S. M. Hughes, A. P. Alivisatos, *J. Am. Chem. Soc.* **2007**, *129*, 10358–10360.
[83] J. Nogués, I. K. Schuller, *J. Magn. Magn. Mater.* **1999**, *192*, 203–232.
[84] J. Nogués, J. Sort, V. Langlais, V. Skumryev, S. Suriñach, J. S. Muñoz, M. D. Baró, *Phys. Rep.* **2005**, *422*, 65–117.
[85] V. Skumryev, S. Suriñach, Y. Zhang, G. Hadjipanayis, D. Givord, J. Nogués, *Nature* **2003**, *423*, 850–853.
[86] A. D. Smigelskas, E. O. Kirkendall, *Trans. AIME* **1947**, *171*, 130.
[87] H. J. Fan, U. Gösele, M. Zacharias, *Small* **2007**, *3*, 1660–1671.
[88] Y. Yin, R. M. Rioux, C. K. Erdonmez, S. Hughes, G. A. Somorjai, A. P. Alivisatos, *Science* **2004**, *304*, 711–714.
[89] Y. Yin, C. K. Endonmez, A. Cabot, S. Hughes, A. P. Alivisatos, *Adv. Funct. Mater.* **2006**, *16*, 1389–1399.
[90] I. Pastoriza-Santos, D. S. Koktysh, A. A. Mamedov, M. Giersig, N. A. Kotov, L. M. Liz-Marzan, *Langmuir* **2000**, *16*, 2731–2735.
[91] R. T. Tom, A. S. Nair, N. Singh, M. Aslam, C. L. Nagendra, R. Philip, K. Vijayamohanan, T. Pradeep, *Langmuir* **2003**, *19*, 3439–3445.
[92] T. Hirakawa, P. V. Kamat, *Langmuir* **2004**, *20*, 5645–5647.
[93] T. Hirakawa, P. V. Kamat, *J. Am. Chem. Soc.* **2005**, *127*, 3928–3934.
[94] J. Lai, K. V. P. M. Shafi, A. Ulman, K. Loos, R. Popovitz-Biro, Y. Lee, T. Vogt, C. Estournès, *J. Am. Chem. Soc.* **2005**, *127*, 5730–5731.
[95] K. W. Kwon, M. Shim, *J. Am. Chem. Soc.* **2005**, *127*, 10269–10275.
[96] K.-W. Kwon, B. H. Lee, M. Shim, *Chem. Mater.* **2006**, *18*, 6357–6363.
[97] H. W. Gu, Z. M. Yang, J. H. Gao, C. K. Chang, B. Xu, *J. Am. Chem. Soc.* **2005**, *127*, 34–35.
[98] X. Wang, X. Kong, Y. Yu, H. Zhang, *J. Phys. Chem., C* **2007**, *111*, 3836–3841.
[99] M. Casavola, V. Grillo, E. Carlino, C. Giannini, F. Gozzo, E. Fernandez Pinel, M. A. Garcia, L. Manna, R. Cingolani, P. D. Cozzoli, *Nano Lett.* **2007**, *7*, 1386–1395.
[100] C. Pacholski, A. Kornowski, H. Weller, *Angew. Chem. Int. Ed.* **2004**, *43*, 4774–4777.
[101] Y. Heng, M. Chen, P. M. Rice, S. X. Wang, R. L. White, S. Sun, *Nano Lett.* **2005**, *5*, 379–382.
[102] R. Buonsanti, V. Grillo, E. Carlino, C. Giannini, M. L. Curri, C. Innocenti, C. Sangregorio, K. Achterhold, F. G. Parak, A. Agostiano, P. D. Cozzoli, *J. Am. Chem. Soc.* **2006**, *128*, 16953–16970.
[103] Y. Li, Q. Zhang, A. V. Nurmikko, S. Sun, *Nano Lett.* **2005**, *5*, 1689–1692.
[104] S. Sun, H. Yu, S. X. Wang, patent US20060053971.
[105] W. Shi, Y. Sahoo, H. Zeng, Y. Ding, M. T. Swihart, P. N. Prasad, *Adv. Mater.* **2006**, *18*, 1889–1894.
[106] G. Shan, L. Xu, G. Wang, Y. Liu, *J. Phys. Chem., C* **2007**, *111*, 3290–3293.
[107] W. Song, Y. Wang, H. Hu, B. Zhao, *J. Raman Spectrosc.* **2007**, *38*, 1320–1325.
[108] V. Randle, *The Role of the Coincidence Site Lattice in Grain Boundary Engineering*, Woodhead Publishing Limited, Cambridge (England), **1997**.
[109] H. Gu, R. Zheng, X. X. Zhang, B. Xu, *J. Am. Chem. Soc.* **2004**, *126*, 5664–5665.
[110] A. D. Dinsmore, M. F. Hsu, M. G. Nikolaides, M. Marquez, A. R. Bausch, D. A. Weitz, *Science* **2002**, *298*, 1006–1009.
[111] C. Pacholski, A. Kornowski, H. Weller, *Angew. Chem. Int. Ed.* **2002**, *41*, 1188–1191.
[112] P. D. Cozzoli, A. Kornowski, H. Weller, *J. Am. Chem. Soc.* **2003**, *125*, 14539–14548.
[113] D. J. Eaglesham, M. Cerullo, *Phys. Rev. Lett.* **1990**, *64*, 1943–1946.
[114] E. Carlino, C. Giannini, C. Gerardi, L. Tapfer, K. A. Mäder, H. von Känel, *J. Appl. Phys.* **1996**, *79*, 1441–1447.
[115] Note added in proof: These very recent results were published during peer review of this Microreview: C. Cheng, K. F. Yu, Y. Cai, K. K. Fung, N. Wang *J. Phys. Chem., C* **2007**, *111*, 16712–16716

Received: September 26, 2007
Published Online: December 14, 2007

